

**AN ARTIFICIAL NEURAL NETWORK BASED
APPROACH FOR MODELING SURFACE
ROUGHNESS IN TURNING HYBRID
COMPOSITE UNDER COMPRESSED AIR
COOLING CONDITION**

By

Mohammad Shahadath Hossain


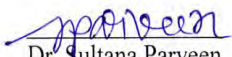
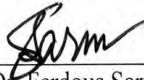

A Thesis
Submitted to the
Department of Industrial & Production Engineering
in Partial Fulfilment of the
Requirements for the Degree
of
M.Sc. in Industrial and Production Engineering

**DEPARTMENT OF INDUSTRIAL & PRODUCTION ENGINEERING
BANGLADESH UNIVERSITY OF ENGINEERING & TECHNOLOGY
DHAKA, BANGLADESH**

October 2015

The thesis entitled as **An Artificial Neural Network Based Approach for Modeling Surface Roughness In Turning Hybrid Composite Under Compressed Air Cooling Condition** submitted by Mohammad Shahadath Hossain, Student No. 0412082020, Session- April 2012, has been accepted as satisfactory in partial fulfillment of the requirement for the degree of M. Sc. in Industrial and Production Engineering on October 31, 2015.

BOARD OF EXAMINERS

- 
1. Dr. Nikhil Ranjan Dhar
Professor
Department of Industrial & Production Engineering
BUET, Dhaka
Chairman
- 
2. Dr. Sultana Parveen
Professor and Head
Department of Industrial & Production Engineering
BUET, Dhaka.
Member
(Ex-officio)
- 
3. Dr. Ferdous Sarwar
Assistant Professor
Department of Industrial & Production Engineering
BUET, Dhaka.
Member
- 
4. Dr. Md. Kamruzzaman
Professor & Head
Department of Industrial & Production Engineering
DUET, Gazipur
Member
(External)

Declaration

It is hereby declared that this thesis or any part of it has not been submitted elsewhere for the award of any degree or diploma.

Mohammad Shahadath Hossain

*This work is dedicated to my
Loving Parents*

*Mr. Mohammad Ali Hossain
and
Mrs. Shafia Khatun*

ACKNOWLEDGEMENT

I express my deepest thanks to Almighty Allah, the most beneficent and the most merciful for making me strong enough to complete this thesis successfully.

I express my profound gratitude to my respected supervisor, Dr. N. R. Dhar, Professor, Department of Industrial and Production Engineering, BUET for his sharing of knowledge, pensive and timely advices, ceaseless support, thoughtful guidance, continuous inspiration, motivation, encouragement and valuable suggestions to complete this work successfully.

I would like to express my gratitude and thanks to the board of examiners Dr. Sultana Parveen, Professor, Department of Industrial & Production Engineering, BUET, Dr. Ferdous Sarwar, Assistant Professor, Department of Industrial & Production Engineering, BUET for their valuable suggestions and guidance.

I acknowledge the help rendered by the Director, DAERS, BUET who provided machine shop facilities whenever required. I am also very thankful to my respected teacher, Prianka Binte Zaman, Assistant Professor, Dept. of IPE, BUET for her extremely generous presence and suggestions during the whole experimental work.

I thank all my helpful colleagues and my departmental Head, Dr. Md. Kamruzzaman, Professor and Head, Dept. of IPE, DUET for his benevolence and inspirations during this thesis work.

Special thanks are due to all the staff members of Central Machine Shop and Machine Tools Lab who have helped a lot whenever required, especially S. C. Das, M. A. Razzak, T. G. Gomes and Manik Chandra Roy for their helps in conducting the experimental work. I am especially thankful to M. A. Karim of Central Machine Shop for his assistance throughout the experimentation.

My family has always been a very important source of support for me. I devote my deepest gratitude to my parents for their love and support throughout my life. Lastly, I offer my thanks to all of those who supported me in any respect during the research work.

ABSTRACT

Modern manufacturing industries are continuously seeking for products which will be light weight, robust, less costly and possess good quality in terms of surface finish and dimensional accuracy. To attain the needs, material engineers are constantly striving to develop new metal alloys as well as composite materials. Composite materials' light weight, high specific strength and high specific modulus are being regarded as some gifted properties which are largely facilitating their applications in different engineering sectors. Kevlar is an organic fiber which possesses excellent specific strength and specific modulus but very poor machinability whereas glass is an inorganic fiber that possesses good machinability along with good blending capability with Kevlar while reinforced in the same matrix. So, to take the advantages of both the contrasting fibers, a hybrid composite can be formed which is going to increase the machinability of Kevlar and retain reasonably good mechanical properties as well. High speed machining is often considered as an accurate manufacturing process for making fiber reinforced plastic (FRP) products and it is established that with high cutting speed and feed productivity increases but high tool wear also takes place hence cost increases. To optimize the situation, different machining environments have been evolved to cut FRPs. Application of conventional cutting fluid, high pressure oil or minimum quantity lubricant is strictly prohibited for machining FRP materials since these machining environments change the FRP composites' properties. In this context, only cryogenic cooling during machining and machining under compressed cooling condition is allowed for FRP materials. It is found compressed air cooling environment has been very effective in machining FRPs when surface roughness and cutting force are taken into consideration.

In this research work, turning operation of hybrid composite i.e. Kevlar and glass reinforced polyester was performed under both dry and compressed air cooling condition. Investigation was carried upon due to compare the performances of two machining environments. Cutting parameters in the machining process were cutting speed, feed and depth of cut and measured responses were surface roughness and cutting force. Finally, a predictive model of surface roughness was developed using artificial neural network (ANN) which has been validated against the experimentally found results.

LIST OF TABLES

Table 3.1	: Experimental conditions	37
Table 4.1	: Data for training and testing	52
Table 4.2	: R^2 and MAPE values between the network predictions and the experimental values using training and test dataset	55
Table 4.3	: Optimal network from ANN	55
Table 4.4	: Summary of the ANN model for optimal ANN architecture for surface roughness prediction of Kevlar and glass fiber reinforced polyester	56
Table 5.1	: Percentage Reduction in main cutting force due to compressed air cooling	60
Table 5.2	: Percentage Reduction in surface roughness due to compressed air cooling	64
Table 5.3	: Actual value of R_a Vs. prediction by ANN	68

LIST OF FIGURES

Fig. 2.1	: Kevlar fiber in fibrous form	33
Fig. 2.2	: Kevlar fiber in the form of fabric	33
Fig. 2.3	: Glass fiber in two different forms	33
Fig. 2.4	: Work material (Kevlar and glass fiber reinforced polyester)	34
Fig. 3.1	: Photographic view of experimental setup	36
Fig. 3.2	: Variation of main cutting force with S_o at different V_c depth of cut 1.0 mm under both dry and compressed air cooling condition	38
Fig. 3.3	: Variation of main cutting force with S_o at different V_c depth of cut 1.5 mm under both dry and compressed air cooling condition	38
Fig. 3.4	: Variation of main cutting force with S_o at different V_c depth of cut 2.0 mm under both dry and compressed air cooling condition	39
Fig. 3.6	: Variation of main cutting force with V_c at different S_o and 1.0 mm depth of cut under both dry and compressed air cooling condition	39
Fig. 3.6	: Variation of main cutting force with V_c at different S_o and 1.5 mm depth of cut under both dry and compressed air cooling condition	40
Fig. 3.7	: Variation of main cutting force with V_c at different S_o and 2.0 mm depth of cut under both dry and compressed air cooling condition	40
Fig. 3.8	: Variation of surface roughness with S_o at different V_c and 1.0 mm depth of cut under both dry and compressed air cooling condition	41
Fig. 3.9	: Variation of surface roughness with S_o at different V_c and 1.5 mm depth of cut under both dry and compressed air cooling condition	41
Fig. 3.10	: Variation of surface roughness with S_o at different V_c and 2.0 mm depth of cut under both dry and compressed air cooling condition	42
Fig. 3.11	: Variation of surface roughness with V_c at different S_o and 1.0 mm depth of cut under both dry and compressed air cooling condition	42
Fig. 3.12	: Variation of surface roughness with V_c at different S_o and 1.5 mm depth of cut under both dry and compressed air cooling condition	43
Fig. 3.13	: Variation of surface roughness with V_c at different S_o and 2.0 mm depth of cut under both dry and compressed air cooling condition	43
Fig. 4.1	: Feed forward neural network	46

Fig. 4.2	: Transfer functions	47
Fig. 4.3	: Schematic diagram of ANN for Surface Roughness	51
Fig. 4.4	: Performance measure of 3-20-1 network	53
Fig. 4.5	: Performance measure of 3-25-1 network	53
Fig. 4.6	: Performance measure of 3-30-1 network	53
Fig. 4.7	: Performance measure of 3-33-1 network	54
Fig. 4.8	: Performance measure of 3-35-1 network	54
Fig. 4.9	: Performance measure of 3-40-1 network	54

CONTENTS

Acknowledgements	v
Abstract	vi
List of Tables	vii
List of Figures	viii
Chapter 1 Introduction	1
1.1 Introduction.....	1
1.2 Literature Review.....	4
1.2.1 Properties of FRP Composite Materials.....	4
1.2.2 Theory and Properties of Hybrid Composite.....	9
1.2.3 Machining of Composite Materials.....	10
1.2.4 Modeling of Surface Roughness.....	19
1.3 Summary of the Review.....	29
1.4 Objectives of the Present Work.....	30
1.5 Scope of the Thesis.....	30
Chapter 2 Material Development	32
2.1 Introduction.....	32
2.2 Development of Hybrid Composite Material.....	32
Chapter 3 Experimental Investigations	35
3.1 Experimental Procedure and Conditions.....	35
3.2 Experimental Results.....	37
Chapter 4 Modeling of Surface Roughness	44
4.1 Introduction.....	44
4.2 Artificial Neural Network (ANN).....	44
4.2.1 Structure of Neural Network.....	45
4.2.2 Types of Neural Network.....	45
4.2.3 Learning Techniques and Error Minimization.....	47
4.3 ANN Input and Output.....	48
Chapter 5 Discussion on Results	57
5.1 Cutting Force.....	57
5.2 Surface Roughness.....	61
5.3 Prediction of Surface Roughness Using ANN.....	65
Conclusions and Recommendations	70
Conclusions.....	70
Recommendations.....	71
References	72

Chapter-1

Introduction

1.1 Introduction

Machining is a process by which works of desired shapes and dimensions are produced by removing extra materials in the form of chips. The operation is done on a machine tool and based on the operation required cutting tools are used to remove the excess materials from the performed work blank. To accomplish this successfully, relative motion between the work and the tool is absolutely necessary. During machining, the material is cut not only due to the variation in speed between the tool and the workpiece but also because of the penetration of tool into the work. Sometimes, the process may become even more complicated when a tertiary movement is provided onto the work blank or work table. Since during machining, material is removed from the work, it is often termed as one of the subtractive manufacturing methods. Machining is very important and sometimes necessary to manufacture products from a broad range of engineering materials. This range can be based on hardness, toughness, modulus of elasticity etc. If hardness is taken into account then machining can be used for cutting hard materials which include hardened high speed steels, tool steels, chilled and chrome irons, some nickel and cobalt-base super alloys etc as well as it can be used to machine comparatively much softer materials such as fiber reinforced composites, plastics etc. The aims and objectives of machining include reduction of cutting force, reduction of surface roughness, reduction of high temperature generation, reduction of dimensional deviation as well as increasing the tool life, increasing the material removal rate (MRR), improving the product quality and as a whole increasing the productivity. To meet the challenges, it is imperative to control the machining responses such as tool life, surface finish, and excessive temperature generation during machining. Different cutting conditions i.e. cutting speed, feed, depth of cut along with different environments e.g. dry, flood cooling using conventional cutting fluid, cryogenic cooling, high pressure cooling, minimum quantity lubrication, compressed air

cooling etc. can produce different results in terms of surface finish, tool life and temperature generation. Apart from machining of metals, machining of fiber-reinforced plastic (FRP) materials has also become very popular despite their relatively high cost. FRP composites pronounce a number of distinguished advantages over conventional engineering materials such as aluminum, steel etc. Among those, higher specific strength, higher specific modulus and higher stiffness are of great significances. They also offer improved fatigue performance as well as superior corrosion resistance in comparison to other engineering materials e.g. steels. For these reasons, they have found their applications in high-performance products which need to be lightweight yet strong enough to work on harsh loading conditions such as aerospace components, automobiles, car bodies, portable bridges, offshore structures, containers, corrosion resistant goods [Tandon et al. 1990]. In order to produce the desired FRP composite products, machining of FRP composite materials has drawn attention among the researchers worldwide. Major constituents of a fiber reinforced composite material are the reinforcing fibers and a matrix. Generally, fiber acts as the load carrying element where the matrix acts the binder for the fibers. Since composite materials are inhomogeneous and anisotropic in nature and protrusion of fibers occurs during their machining, the desired surface finish is often harmed. So, it has become a challenge for the researchers to machine composite materials while keeping the surface roughness down to minimum as well as dimensionally accurate.

Dry machining of steels and composites are often not employed because of the generation of very high cutting force and excessive temperature. The machined surface ultimately possesses poor surface finish as well as smaller tool life is obtained. So, in order to reduce the temperature and cutting force in the chip tool interface, application of additional cooling and lubricity is extremely important. So, as an alternative solution, the application of conventional cutting fluid in the machining zone has long been employed. In the case of machining steels, cutting fluid have been successful in protecting the work blank from reacting with the environment and it also reduces the cutting force as well as temperature in the cutting zone. Despite their number of advantages, cutting fluid has some disadvantages too. Dhar et al. [2007] stated that, although cutting fluid promotes technological advantages, their negative effects have been questioned since they can be environmentally threatening and may cause health-related problems. Also, conventional machining under flood cooling environment involves higher manufacturing cost as well as

poses serious environmental and health hazards. Again, their safe disposal without harming the surroundings is often too difficult to achieve.

As a remedy, the manufacturing fraternity is constantly striving to decrease the costs associated with machining and increase the quality of the machined parts along with the reduction in health and environmental hazards. So, the demand of green environment is rapidly increasing [Dureja et al. 2015]. It has been confirmed that application of conventional cutting fluid has a serious impact on both health and environment [Tai et al. 2014, Oliveira et al. 2012]. Again, it is also very well established that in machining of FRP composite materials; supply of cutting fluid, cutting oil or any kind of liquid in chip tool interface can deteriorate FRP's properties. So, as a much greener approach and keeping health and environment in thoughts, compressed air cooling has emerged in machining composite materials. Modeling of the different machining responses e.g. modeling of tool wear, temperature generation, cutting force and surface roughness have also been a matter of great attention for the researchers. As surface roughness of the produced part is ultimately the main quality evaluation parameter, the modeling of surface roughness has also been thoroughly studied by the researchers worldwide. Different techniques such as response surface methodology (RSM), multiple regression analysis (MRA), adaptive neuro fuzzy based inference system (ANFIS), artificial neural networking (ANN) etc. are there to predict surface roughness reasonably accurately. Researchers like Escalona and Maropoulos [2010], Asilturk [2012] used ANN to predict the surface roughness of the machined part. Research in this area is still going on in a rapidly growing manner.

The whole thesis can be divided into three main parts. In the first part, development of the desired hybrid composite material for this research work will be presented. In the second part, machining investigation of the machining of composite material will be presented along with the variation of cutting force and surface roughness with different cutting conditions and machining environments. In the final part, an artificial neural network (ANN) model for predicting surface roughness of the machined part will be presented along with its validation. A review of the literature regarding the work is presented in this section below and this will also give a glimpse of the latest developments in the area concerned with the present work.

1.2 Literature Review

From most of the research works, it can be affirmed that surface finish, cutting force, temperature generation, tool wear as well as dimensional accuracy of the produced work blank are the major concerns regarding the machinability study of the developed work material. Different techniques and systems have been developed to reduce the cutting force and cutting temperature in order to increase tool life and surface finish. Machining environments such as flood cooling, cryogenic cooling, minimum quantity lubrication (MQL) and as an environment friendly approach compressed air cooling have been emerged to machine steels across the globe. Unlike steels, the machining responses gained from machining a FRP composite material are quite diversified and these depend on the composition of different constituents, manufacturing method and accuracy of the composite material as well. This reason has led the researchers to study FRP composite materials' properties thoroughly.

1.2.1 Properties of FRP Composite Materials

Fiber-reinforced plastic (FRP) materials such as carbon fiber-reinforced plastics, glass fiber-reinforced plastics and Kevlar fiber-reinforced plastics are finding an escalating use in a wide variety of engineering sectors these days. These materials offer a number of distinguished advantages over conventional engineering materials e.g. aluminum, steel etc. However, they often suffer from some serious limitations. One of the most prominent among those is their response to localized impact loading where impact response is an essential parameter for judging the feasibility of a composite material for high strain rate engineering applications [Marom et al. 1978]. They conducted experiments with hybrid composites with different arrangements of carbon and Kevlar fiber reinforcing epoxy matrix. It was found that significant positive hybrid effect in impact energy when the hybrid was formed as sandwich with Kevlar layer placed as the outside layer. The result also ascertained, layer stacking sequence was the most common parameter on the generation of hybrid effects. Again from their experiment, it was clearly observed that delamination was the most salient fracture mechanism of the hybrid composite and in each of the failure event carbon layer preceded Kevlar layer.

Bunsell [1975] conducted experiments on Kevlar-49 fiber. The experiment dealt mainly with tensile, creep and fatigue behavior of Kevlar-49 fiber. It was found that during the experiment, the fiber survived under steady load but failure occurred due to creep when loaded very near to its tensile breaking load. It was also noticeable that the fiber failed under fatigue and its fatigue lifetime depended on the amplitude of the applied cyclic load and maximum load to which the fiber was cycled as well. Hearle and Wong [1977] investigated the flexural fatigue and abrasion properties of Kevlar-29, glass fibers and carbon fibers. Kevlar-29 fibers were found to perform well on those experiments as they survived the relatively high bending strains by yielding in axial compression. Kevlar-29 fibers were found to be less abrasion resistant than carbon and glass fibers and that phenomenon may be attributed to their low radial strength. Studying fracture morphology, it was affirmed that axial splitting was the main reason behind their failure which indicated low strength with respect to the normal to fiber axis.

Ho and Suh [1979] investigated the effect of fiber orientation on friction and wear of unidirectionally oriented graphite fibers reinforced epoxy, unidirectionally oriented Kevlar-49 reinforced epoxy and poly tetrafluoro ethylene based material. According to their findings, in graphite-fiber epoxy composites, both the wear and friction coefficient was minimum when the orientation of the fibers was normal to the sliding surface. In the case of Kevlar-epoxy composites the wear rate was also minimum when the orientation of the fibers was normal to the sliding surface but the friction coefficient was maximum. In glass fiber-Molybdenum sulfide- poly tetrafluoro ethylene composites, wear was minimum when the orientation of the fibers was normal to the sliding surface.

Time dependent strains of Kevlar 49 fiber and Kevlar 49-cement based composite were studied by [Walton and Mazumder 1983]. The study required a long period of time and it had been confirmed, creep strains in Kevlar 49 fibers were low at room temperatures. With increasing stress, creep strain decreased. Again, creep-time for both fibers and composite were related by a power function. By using that relationship, long term strains could also be predicted. The interface between the fiber and the matrix plays a very important role in FRP materials. The strength of interface also affects the crack propagation. Researchers have shown that, if the interface is weaker than matrix then a crack formed perpendicular to the fiber can propagate parallel to them along the interface

[Mittelman and Roman 1990]. They studied and conducted experiments to determine the tensile properties of real unidirectional Kevlar/ epoxy composites. They investigated the mechanical behavior, tensile strength and failure modes in unidirectional Kevlar/ epoxy composites for different fiber volume fractions V_f . The load was applied parallel to the fiber and the V_f range was 0.26 to 0.73. It was found that the measured tensile strengths deviated from the expected values calculated from the rule of mixtures (ROM). The difference between the calculated and the achieved tensile strength was least when V_f was 0.5. When V_f was less than 0.5, they explained the deviation with non homogenous fiber spread and distribution of fibers. When V_f was greater than 0.5, the deviation was explained with increasing lack of matrix between the fibers.

Ganczakowski and Beaumont [1989] studied the behavior of Kevlar fiber reinforced epoxy (KFRP) laminates under static and fatigue loadings. The specimen used in the experiments were laminates made from 3M Scotchply SP 328 Kevlar/epoxy resin prepreg containing 50% of fibers by volume. The nominal ply thickness was 0.22 mm. Coupons of dimensions 200 mm \times 25 mm, were stored in sealed plastic bags at room temperature. Tests were carried out under ambient conditions. After conducting the experiment they found, under tensile loading, Kevlar fibers and unidirectional KFRP laminates showed an increase in longitudinal modulus. This stiffening effect occurred under both cyclic and long-term static loading and depended on time rather than load cycles, and was reversible on relaxation. Under fatigue loading, the modulus of cross-ply KFRP laminates depended on a combination of the stiffening effect of the longitudinal plies and the damage due to matrix cracking in the transverse plies. The modulus behavior of these laminates under fatigue loading is therefore more complicated than that of glass fiber reinforced plastic (GFRP) or carbon fiber reinforced plastic (CFRP). Wu and Yeh [1992] focused on the experimental verification of mathematical model to show the effect of initial fiber misalignment on the compressive response of Kevlar- epoxy composites. Due to the considerable amount of variations of properties among the components, FRPs are very much sensitive to fiber misalignment and waviness. Deviation of the fiber direction in the laminae from the planned direction is known as misalignment. According to their observation, the failure mode was predominant due to the formation of kink band. Again, the distribution of initial fiber displacement followed a two- parameter Weibull distribution with large variability.

Wang et al. [1995] studied the mechanical properties of fiber glass and Kevlar woven fabric reinforced composites. Their study aimed at characterizing the mechanical behavior of fiber glass and Kevlar woven fabric reinforced epoxy composite laminates under various conditions. Epoxy resin was used as the matrix material. Fiber glass fabrics were of two kinds, style 1597 and style 1800, and two types of Kevlar 49 fabrics, style 354 and style 383. The double cantilever beam (DCB) test, the uniaxial tensile test, the three point flexural test, the compression test and short beam shear (SBS) test were performed on the specimens in order to figure out different mechanical properties of the work specimen. According to their findings, fracture mechanisms were mainly (i) fiber rupture, (ii) fiber pull-out, (iii) fiber debonding, (iv) Kevlar fiber fibrillation, (v) multiple fracture of matrix resin and (vi) possible matrix plastic deformation. According to their findings, fiber type showed strong effect on the mechanical behavior, particularly the load-deformation responses of the composites under tension, flexure, compression, short beam shear and double cantilever beam test conditions. Because of Kevlar fibers' poor transverse and shear strengths; Kevlar fiber reinforced composites exhibited a high degree of nonlinearity and lower strength in flexure, compression.

Many researchers have shown that the compressive behaviors of the fibers are dependent on the tensile modulus of the fibers. Some have found compressive behavior to be independent of the tensile properties rather dependent on molecular interactions [Andrews et al. 1997]. In their study, they applied four point bending beam method to figure out the compressive properties of a number of distinguished aramid fibers using a combination Raman spectroscopy and optical microscopy. They noticed that the compressive strength of aramid fiber was much lower than tensile strength. According to their observation, the compressive failure of aramid fibers initiated where the stress strain curve deviated from linearity and indicated the onset of molecular yielding. Also, the compressive failure was characterized by the formation of visible kink band.

Fibers in a composite material get damaged when exposed to thermal environment either intentionally or accidentally during the fabrication of the fibers or while in use [Yue et al. 2000]. They studied whether any thermally induced detrimental effect occurred to Kevlar 29 fibers during the fabrication process of the composite. They applied thermal aging treatments on Kevlar 29 yarns under both atmosphere and vacuum

environments at temperatures of 100 °C to 300 °C for durations from 2 h to 8 h. It was found that both the tensile strength and tensile strain decreased with the increase in treatment temperature. While treatment was done at constant temperature, the heating duration had no effect on tensile strength and tensile strain. Under the experimental conditions, it was observed that Young's modulus was unaffected by the heat treatment process. Again, it was also found that heat treatment in vacuum did not have any effect on tensile strength on Kevlar 29 fiber.

Moreover, researchers have found it of major importance to understand the dynamic mechanical behavior of fibers and fiber bundles. Few study results have been reported on the dynamic mechanical properties of Kevlar aramid fibers and fiber bundles [Wang and Xia 1998]. They studied the effects of strain rate on the mechanical behavior of Kevlar-49 fiber and based on experimental results the validity of the bimodal Weibull distribution statistical constitutive model of Kevlar-49 was also verified. They found that Kevlar-49 fibers were sensitive to strain rate but in comparison to glass fiber bundles the degree of sensitivity of Kevlar-49 was not very severe. Based on experimental results, it was also proved that the method of determining the mechanical properties and Weibull parameters of fibers by means of fiber bundle tensile tests were also feasible and reliable. Wang and Xia [1999] also studied the strain rate and temperature dependence of Kevlar fiber. They measured the dependence of Kevlar fiber for three different strain rates and five different temperatures. It was noticed that Kevlar-49 fiber had sensitivity to strain rate and temperature. Its initial modulus of elasticity, strength and breaking strain increased with increasing strain rate for a constant temperature. For fixed strain rate, with increasing test temperature the initial elastic modulus decreased and breaking strain increased. Again, It was also found that for different temperatures and strain rates for Kevlar-49 under tensile impact loading the constitutive model considering strain rate and temperature dependence can be universally applied to characterize the combined effects of strain rate and temperature on the mechanical behaviors of the fibers.

Kevlar fabric has also found its applications in making body armor [Kang et al. 2010]. In their study, they prepared shear thickening fluid (STF) impregnated fabric composites and investigated their mechanical properties and stab resistance to use that as a body armor material. It was observed that the frictional resistance between a spike

impactor and the fumed silica/ Kevlar composite fabric increased with increasing the number of fabric ply. In the case of neat Kevlar fabric, the result hardly changed with the changing number of plies. Again, excellent improvements in puncture resistance were observed under high speed loading. It was also found that the STF addition did not damage the flexibility of the STF treated Kevlar fabric in comparison to neat Kevlar fabric.

1.2.2 Theory and Properties of Hybrid Composite

When a matrix is reinforced with a multiple number of fibers, then the developed composite is known as hybrid composite. Any deviation of mechanical properties of hybrid composites from the rule of mixture (ROM) is defined as ‘_hybrid effect’. Another definition identifies the hybrid effect as the difference between the failure strain of the low elongation fiber in a hybrid composite and that in a pure low elongation (LE) fiber composite. A positive hybrid effect suggests that the property is above the ROM value or a greater failure strain in LE fibers is observed, while a negative hybrid effect is the property below the ROM value. The performance of hybrid composite depends not only on the properties of fibers and matrix but also on the interfacial properties between fiber and matrix [Qiu and Schwartz 1993]. They worked with Kevlar-149 fiber and S glass fiber reinforcing epoxy matrix and found a positive hybrid effect in the case of failure strain but a negative one in the case of strength. It was also observed that Kevlar-149 fibers exhibited much higher strengths in microcomposites than in a single fiber tensile strength.

Kevlar fiber in combination with carbon fiber has also been used as sandwich composite. The attractive features of these composites have made them suitable for various applications. They are favored for their high specific strength, corrosion resistance, tailorability and stability. Gustin et al. [2005] investigated impact, compression after impact and tensile stiffness properties of carbon fiber and Kevlar fiber combination sandwich composite. In the experiment, different sample’s impact side facesheet had different combinations of carbon fiber/ Kevlar fiber but the bottom facesheet was entirely made of carbon fiber to maintain the high overall flexural stiffness of sandwich composite. They found with a little variation the compressive strength decreased with increased impact energy. The major mode of failure was either facesheet crushing, cracking or delamination. The addition of Kevlar to the facesheet improved maximum absorbed energy and average maximum impact force.

1.2.3 Machining of Composite Materials

Due to the heterogeneity and anisotropic properties of composite material, it is always difficult to machine them. In many fabrication processes, machining is avoided but many a time it is almost impossible to ignore machining. As, there are large number of variables associated with the responses of machining process such as fiber orientation, matrix properties; data on the machinability of FRP is scarce. Some of the common problems which occur during the machining of aramid fiber reinforced plastics are

- delamination of the work material
- differential expansion and thermal conductivity between the fibers and matrix material results thermal damage
- machining of tough aramid fibers results in a irregular surface, damaging the cutting tool significantly.

During machining whenever the cutting tool gets subjected to severe load fluctuations cutting flanks get damaged [Santhanakrishnan et al 1989]. They examined the mechanism of metal removal during machining of glass fiber reinforced plastic (GFRP) and type of tool wear. The mechanism of tool wear was explained with help of a scanning electron micrograph (SEM). The tool material used in the experiment was high speed steel (HSS) with varying amount of cobalt. It was observed that machining of GFRP was associated with plastic deformation, shearing and rupturing of the fiber. Again, Santhanakrishnam et al. [1988] affirmed that when a cutting tool wedge entered the workpiece, a phenomenon similar to indentation took place. If the work blank were a ductile material, it would be plastically deformed and sheared but in the case of brittle material, it might undergo cracking due to rupture. In general, a combination of plastic deformation, shearing and bending rupture would take place during machining of FRP composites. They performed various face turning operations to figure out the machinability characteristics of FRP composites. The work materials used in the experiments were glass fiber reinforced plastic (GFRP), carbon fiber reinforced plastic (CFRP) and Kevlar fiber reinforced plastic (KFRP). From their studies it was found, the brittle carbon fibers got crushed and fractured sharply during CFRP machining and gave a surface of better quality compared to other FRP composites. KFRP exhibited poor surface finish due to the irregularity caused by delaminated, dislocated and strain ruptured tough

Kevlar fibers. Due to their higher toughness, Kevlar fibers sheared during machining. Again because of the increase in plowing component of cutting, cutting force during KFRP machining is larger in comparison to machining of other FRP composites.

Bhattacharya et al. [1993] studied cryogenic machining of Kevlar composites. It was evident that in cryogenic environment the fiber matrix behaved in a much more rigid fashion and it produced very little amount of bent and pulled out fibers. In their experiment, the used work material was Kevlar 49/epoxy rods of 20 mm diameter and 600 mm length with longitudinal continuous fiber orientation and the fiber volume fraction was 40%. The depth of cut used in the experiment was 1.0 mm and the feed rate was 0.05 mm/rev. Two cutting speeds were used during the experiment and they were 100 m/min and 50 m/min. Three ranges of workpiece temperatures were used while machining; range 1: -195°C to -185°C , range 2: -135°C to -105°C and range 3: -75°C to -60°C . According to their findings, tool wear got readily reduced but due to the continual rubbing of loosened fibers, chip notching temperature increased in tool workpiece interface which led to increase the cutting force. Having noticed that, it was also found that generation of cutting force was much lower in comparison to metallic materials. With the increase in cutting force, surface roughness increased that deteriorated surface integrity. The degrees of fiber pull out and fiber protrusion depended on various cutting parameters. Under cryogenic condition, both the cutting speed used in the experiments produced desired surface finish. However, the lower cutting speed tended to produce better quality surface even though tool wear slightly appeared to be of higher growth.

Lin and Chen [1996] performed drilling operation on a fiber reinforced composites. The objective of the experiment was to learn the effects of increasing cutting speed on drilling characteristics of FRP. They examined the effects of cutting speed on average thrust force, torque, tool wear and hole quality with two kinds of drill bit one was twist drill and other was multifaceted drill. They found the results such as average thrust force increased with increasing cutting speed for both kind of drill. Average torque increased in little amount with increasing cutting speed for multifaceted drill but opposite occurred in the case of twist drill. The average torque appeared greater for multifaceted drill than twist drill in the case of low cutting speed but in high speed cutting, average torque for multifaceted drill was smaller than twist drill's. It was also observed that, thrust

force was increased with the increase in drilled length but the effect of cutting speed was much more significant than the effect of drilled length.

Persson et al. [1997] investigated the effects of hole machining defects on strength and fatigue life of composite laminates. Dry test specimens were subjected to pin loading and uniaxial compressive loading at room temperature. Non-destructive examination (NDE) methods were used to detect the defects caused by the hole machining processes. The specimen used in the experiments was, laminates were fabricated from the toughened carbon/epoxy HTA7/6376 system. The stacking sequence of the laminates was $[(\pm 45/0/90)_3]$. After conducting the machining investigation they found, NDE showed the extent of hole generation defects. No damage was evident around holes in the KTH specimens,; but in the case of Dagger specimens, the defects extended from the edge of the hole to a depth in the laminate of nearly a quarter of the hole radius; around holes in the PCD specimens, the defects extended from the edge of the hole to a depth in the laminate nearly equal to the hole radius.

Bhattacharya and Horrigan [1998] studied drilling of Kevlar composites with normal and modified drill bit (negative point angle) under both ambient and cryogenic condition. According to their findings, KFRP laminates could be successfully machined with HSS drill bits at available drill speeds containing negative point angle and sufficiently large clearance angle. The goodness of machining largely depended on the temperature at which it was carried out. Average hole quality and dimensional accuracy were improved by using modified drill bit of a large helix angle. Again, the application of liquid nitrogen at the drilling site dramatically improved the hole quality and tool performance.

Rahman et al. [1999] studied the machinability of carbon fiber reinforced composite. The experiment that they conducted was limited to the turning of a cylindrical shaft. The test specimens were carbon fiber reinforced epoxy composite. Two types of specimens were fabricated, namely short carbon fiber epoxy composites and long carbon fiber epoxy composites. The purpose of the study was to investigate how best the material could be machined using different tool inserts and varying cutting condition i.e. cutting speed, depth of cut, and feed rate. Cubic boron nitride (CBN) and tungsten carbide (WC) were used as the cutting tool material. The design of experiment (DOE) was used to investigate the relative effects of input parameters on tool wear and surface finish. From

the machinability study of CFRP, it was found that thermosets i.e. CFRP were more brittle and possessed less capability for plastic deformation than thermoplastic and their chips tend to fracture earlier. Discontinuous chips in powder form were found during machining. Short fiber CFRP exhibited no particular trends and this could be attributed to the random fiber orientation in the matrix, and the fracture mechanism being quite complicated, with shearing in the perpendicular direction and buckling in the parallel direction. It was also found, regardless of the chip formation mechanism higher cutting forces higher feed rates produced higher feed rates. However, the cutting force fluctuates due to two phases of materials being present in CFRP composites.

Teti [2002] studied the machining of composite materials by conducting turning, milling and drilling on metal matrix composite (MMC), ceramic matrix composite (CMC) and plastic reinforced composite (PMC). It was found that, among the possible wear mechanisms; abrasion, surface damage and sometimes adhesion were significant in machining of FRP materials. Because of their extremely abrasive nature, glass and carbon fibers showed a strongly abrasive behavior. Since, aramid fibers possess low heat conductivity and ductile characteristics, they impaired the tool. In machining GFRP and CFRP, it was the cutting tool material that governed the tool selection. But when aramid fiber reinforced plastics (AFRP) was taken into consideration, it was the tool geometry that dictated the choice of cutting tool. Their work also provided a comparison between carbide tools, coated carbide tools and polycrystalline diamond (PCD). All of those tools yielded good results in terms of tool wear and tool life during the machining of GFRP and CFRP, although the wear for these tool materials was considerably different. It was believed that PCD could be an economical alternative to carbide in machining FRP despite the much higher purchase cost because tool life was longer and higher processing speeds could be used. For the same machining operation, tool wear found to be higher for thermoplastic matrix FRP rather than for thermoset matrix FRP. In machining thermoplastic matrix FRP composites, satisfactory results were obtained only when PCD was used as tool material. MMC machinability was critically affected by the reinforcement and matrix hardness. It was also observed that higher hardness shortened the tool life critically.

Brinksmeier and Janssen [2002] studied the drilling of multi-layer composite materials consisting of CFRP, titanium and aluminum alloys. In one of their studies, they

used workpiece consisted of aluminum alloy and CFRP while in the other experiment the multilayer workpiece were made by Titanium alloy (TiAl6V4), Aluminum alloy (AlCuMg2) and CFRP. For both the experiment, cutting speeds were 10 m/min and 20 m/min., feed was kept constant at 0.15 mm. Cutting tools used for the experiments were a conventional drillbit and a modified step drill bit. Both with helix angle 30° and point angle 120° . The conventional drillbit was uncoated but the modified one was uncoated, TiB_2 and diamond coated consecutively. The objectives of the experiments were to investigate the effects of tool geometry and drilling parameters on cutting forces and hole quality. It was found that while drilling CFRP/Al, holes with small diameter tolerances were difficult to drill. The modulus of elasticity (E) of the materials caused different elastic deformations and therefore varying tolerances along the entire hole. Additionally, the chip transport through the hole as well as build-up cutting edges of aluminum at the primary and minor cutting edges combined with increased tool wear affect the hole quality. While drilling Al/Ti/CFRP, the influence of chip transport through the chip grooves and adhesion tendency of titanium chips on the cutting edge leads to severe damage to the surface quality. When tool wear was in concern, it was clearly evident that while drilling Al/CFRP workpiece with modified drillbit. Investigations showed that, friction contact at the rake and the flank faces while drilling Al alloy/Ti alloy/CFRP led to unfavorable mechanical and thermal loads on the cutting edge which increased tool wear, tool life index was very low for both the drill bits.

Sonbaty et al. [2004] performed drilling operation to test the machinability of GFR-epoxy composite. The parameters used in the experiment were cutting speed, feed, drill size and fiber volume fraction. The prime objective of the research was to investigate the influence of parameters on thrust force, torque and surface roughness of the desired product. The work material used in the experiment was randomly oriented glass fiber reinforced epoxy matrix with varying fiber volume fraction. Values of fiber volume fractions ($V_f = 0\%$, 9.8%, 13.6% and 23.7%). The composite laminates, with 8.5 ± 0.1 mm thickness, were fabricated using hand layup technique. Drilling operations were conducted using standard HSS twist drillbits. The drilling processes were carried out on epoxy resin and glass fiber reinforced epoxy composite (GFREC) with back plate under the following cutting conditions. In order to study the effects of speed and feed on thrust force and torque, five different spindle speeds (218 rpm, 455 rpm, 634 rpm, 875 rpm and 1850 rpm)

and three different feeds (0.05 mm/rev., 0.10 mm/rev. and 0.23 mm/rev.) were used. The machining was done on GFREC specimens of various V_f ratios, $V_f = 0\%$, 9.8%, 13.6% and 23.7%. Again, to study the effects of drill diameter on thrust force and torque six different drill diameters ($D = 8$ mm, 9 mm, 10 mm, 11 mm, 12 mm and 13 mm) were chosen at 875 rpm spindle speed along with three different feeds ($f = 0.05$ mm/rev., 0.10 mm/rev. and 0.23 mm/rev.). After conducting series of experiments, they inferred that the behavior of thrust force and torque during the drilling cycle was quite varying. As an example, at low speed ($n = 218$ rpm) and investigated feeds ($f = 0.05$ mm/rev., 0.1 mm/rev. and 0.23 mm/rev.). It was found that, for epoxy resin, increasing cutting speed had not any considerable effect on thrust force. On the other hand, torque decreased with increasing cutting speed. For all the materials (epoxy matrix and GFREC), the thrust force and torque was increased with increasing the feed. The thrust force and torque of GFREC were decreased with increasing cutting speed and increased with increasing drill diameter and V_f ratios. Moreover it was also observed that, the cutting speed and feed had no significant effect on surface roughness of epoxy resin and for GFREC, the surface roughness was improved by increasing cutting speed and fiber volume fraction. The drilled holes of GFREC had higher roughness with lower V_f value and lower feed than that drilled at higher feed. Specimens with high V_f ratio have a contrary behavior. Surface roughness was found to have been significantly affected by drill diameter combined with feed.

Singh and Bhatnagar [2006] investigated the drilling of uni-directional fiber reinforced composite laminates. They used three different cutting speeds of 750 rpm, 1500 rpm and 2250 rpm along with three different feeds of 10 mm/min, 15 mm/min and 20 mm/min. The cutting force, torque and thrust force were measured in the experiment. They operated the experiment using four different types of drillbits. They figured out that higher thrust and the torque values were found for the 4- facet drill point geometry and therefore the 4-facet drill could not be recommended for drilling laminated UD-GFRP composites. The thrust and torque responses were found to be lower for 8-facet and Jodrill than the other two geometries. While drilling-induced damage was in concern, an elliptical zone was found with the major axis of the ellipse lying in the direction of the fibers. The damage depended on the speed/feed ratio, providing maximum value at higher cutting speeds. Contrary to the general belief, drilling-induced damage was not correlated with the thrust force trends for all the drill geometries; however, it matched with the torque trend

and they inferred that the theoretical models assuming thrust as the main contributor of damage was not correct and might lead to ambiguous algorithm development.

Abrao et al. [2007] studied a number of articles on drilling of glass fiber reinforced epoxy and carbon fiber reinforced epoxy and found some noticeable phenomena. Both conventional high speed steel twist drill bit was used as much as cemented tungsten carbide drills during the experiments. The principal factors that were used to evaluate the performance of the process were the damage caused at the drill entry and exit and the roughness on the wall of the hole produced. The following conclusions could be drawn with regard to the drilling of fiber reinforced plastic materials. It was noticed that feed rate was the governing factor in the case of surface finish of the hole mostly but based on the design of the drillbit its effect could also be negligible in some cases. Despite the fact that the damage of work material was frequently measured in terms of delamination, some researchers also divided damage in multiple categories such as delamination at drill entry, geometric defect of the cutting tool, temperature oriented damage, delamination at drill exit.

Davim and Mata [2007] made a comparative evaluation of turning between reinforced and unreinforced polyamide. As unreinforced polymer, polyamide 6 (PA6) and as reinforced polymer, polyamide reinforced with glass fiber (PA66-GF30) was used in the experiment. In both of the cases, the workpiece diameter was 50 mm along with the length of 100 mm. Three levels of cutting velocity 200 m/min., 100 m/min. and 50 m/min. and three levels of feeds 0.05 mm/rev, 0.10 mm/rev and 0.20 mm/rev were chosen for the experiment. According to their findings, the effect of glass fibers on composite PA 66-GF30 led to higher values of cutting forces, friction angle and normal stresses in comparison to polymer PA 6. PA 6 presented greater values of shear stresses and chip deformation than PA 66-GF30.

Isik [2007] performed machining investigation on glass fiber reinforced plastic. The work material used in the experiment was glass fiber reinforced polyester. Turning operation was done on the workpiece where three levels of cutting speeds, three levels of feeds and three levels of depth of cuts were used during the investigation. The cutting tool used in the experiment was CERMET tool. The cutting speeds were 170 m/min., 188 m/min. and 206 m/min., the feeds were 0.20 mm/rev., 0.25 mm/rev. and 0.30 mm/rev. and

the used depth of cuts were 0.15 mm, 0.20 mm and 0.25 mm. According to their findings, surface roughness was decreased with increasing cutting speed whereas it was increased with increasing feed rate. Again, surface roughness increased with increasing rake angle and decreased with increasing tool radius.

Bhushan et al. [2010] performed turning operation on SiC reinforced 7075Al alloy with different cutting conditions to observe the effect of cutting condition on machined surface. Tungsten carbide (WC) and polycrystalline diamond (PCD) tools were used in the experiment. The cutting speeds chosen for the experiments were 180 m/min., 200 m/min., 220 m/min. and 240 m/min., feed rates were 0.10 mm/rev., 0.20 mm/rev., 0.30 mm/rev. and 0.40 mm/rev. whereas the depth of cuts were 0.50 mm, 1.0 mm, 1.5 mm and 2.0 mm. They concluded that surface roughness of Al alloy was lesser in comparison to Al alloy composite during turning regardless of the tool insert. Wear of carbide and PCD inserts were less during turning of Al alloy as compared to Al alloy composite. To keep the surface roughness optimal, it was recommended that turning operation on Al alloy composite by carbide insert should be carried out at, cutting speed within the range of 180 m/min to 220 m/min, feed rate within range of 0.1 mm/rev. to 0.3 mm/rev., and depth of cut was within range of 0.5 mm to 1.5 mm. For getting flank wear in the carbide insert minimal, machining should be carried out at cutting speed of less than 200 m/min, feed rate of 0.1 mm/rev, and depth of cut of 0.5 mm.

Azmi et al. [2012] performed machinability study of GFRP during end milling. The sample workpiece used in the experiment was GFRP composite panels using vacuum-assisted resin transfer molding, resulting in high laminate quality, i.e. higher volume fraction and less number of voids. The laminates consisted of 16 layers of uni-directional E-glass fiber with epoxy resin as the matrix material. The laminates were cut into plates with a size of 200 mm× 135 mm× 6 mm using a water-cooled diamond saw for the subsequent machining experiments. Fiber volume fraction (V_f) was regularly monitored according to ASTM D3171-09 in order to ensure the consistency of laminate quality with an average value of carbon fiber epoxy composites. Carbon fiber epoxy composites V_f to be 0.52. The machining conditions of the experiments were three levels of feed rates low 500 mm/min., 750 mm/min. and 1000 mm/min.; The used depth of cuts were 1.0 mm, 1.5 mm and 2.0 mm; the spindle speeds were 3000 rpm, 4000 rpm and 5000 rpm. Their

findings included that feed rate had the most dominant role in influencing the surface roughness (R_a), followed by spindle speed with each factor contributing 67% and 19%, respectively. The effect of depth of cut had been found to be negligible. The governing effect of feed rate on surface roughness (R_a) might be attributed to the different mechanisms of chip formation at various feed rates. It was also important to note that R_a value alone might not be sufficient enough to describe the surface finish of FRP composites due to fiber protrusion. SEM images were used to verify the surface integrity and morphology of the machined laminates. The tool life performance of the K20 end mill cutter was mainly dominated by the feed rate (85%) and spindle speed (11%). The resultant machining force, F_m , was considerably affected by feed rate and depth of cut at 54% and 45% contributions respectively.

Dandekar and Shin [2012] studied a number of articles concerning the machinability and modeling of machining of composite materials. According to the article, a group of researchers conducted orthogonal machining tests on carbon fiber-reinforced polymeric (CFRP) composites and observed the chip formation, surface quality and cutting forces for two fiber orientations: perpendicular (90°) and parallel (0°) fiber orientations relative to the cutting direction. Two noticeable results were found, the chip formation mechanism was a series of fractures observed in the fibers and a rougher surface was observed from 90° fiber orientation samples as compared to 0° fiber orientation. Another group of researchers studied machining of fiber reinforced polymer (FRP) based composite materials, by a number of processes such as drilling, turning, milling and water jet cutting. In their work, various damage phenomena were observed in detail which occurred during machining of fiber reinforced composites were fiber debonding, spalling, cracking of the matrix, fiber failure and fiber pull out. Again, in another study the researchers described the chip formation process in the machining of a GFRP composite. They observed chip formation was highly dependent on the fiber orientation with respect to the cutting direction and observed metal-like chip formations while machining the composite with a thermoplastic matrix as opposed to a thermosetting resin polymer matrix.

In another study, the research personnel conducted orthogonal tool wear tests on CFRP specimens. Fiber orientation angle and cutting speed were found to be the major contributors to the flank wear. The tool wear was caused due to the very abrasive nature of

the carbon fiber. It was also shown that fiber orientation and feed affected the surface roughness more than cutting speed. A study was conducted by some researchers, on the influence of fiber orientation on the cutting forces and fiber pull-out in GFRP. They concluded that the tool with a positive rake angle resulted in the least amount of damage in the machined composite and lower cutting force. Tests were conducted on fiber orientations of 45° , 90° and 135° , measured in a counterclockwise direction from the cutting direction. Other studies also addressed the effect of cutting parameters, tool geometry and fiber orientation on the sub- surface damage observed in machined samples. The results once again corroborated earlier findings on the effect of fiber orientations on the damage: lower cutting forces for higher fiber orientations, consequently resulting in less damage. It was shown from some works that the cutting force and the sub- surface damage increased with increasing fiber orientation while the rake angle had no or minimal effect on the cutting forces and the observed damage.

1.2.4 Modeling of Surface Roughness

In machining of parts, surface quality is one of the most specified customer requirements. Major indication of surface quality on machined parts is surface roughness. FRPs contain two phases of materials with drastically distinguished mechanical and thermal properties, which brings in complicated interactions between the fiber and the matrix during machining. The material anisotropy resulting from fiber reinforcement heavily influences the chip formation and other machinability indices during machining [Komanduri et al. 1991].

It is considered that the product quality increases with a decrease in surface roughness. Controlled parameters such as cutting condition and non-controlled parameters such as work-piece non-homogeneity, tool wear, machine motion errors, chip formation and other random disturbances; all have effects on surface roughness. It has been shown that both controlled and non-controlled parameters cause relative vibrations in the cutting tool and work-piece [Brezocnik and Kovacic 2003]. Karayel [2009] contended that the difficulty in controlling roughness is due to the intrinsic complexity of the phenomena that generates during its formation. For these reasons, roughness modeling has become not just an especially defying business but an area of great interest for research.

Chen and Savage [2001] used fuzzy net-based model to predict surface roughness under different tool and work piece combination for end milling process. The input parameters included cutting speed, feed, depth of cut, vibration, tool diameter, tool material, and work piece material for the fuzzy system. While validating the model it was found that the predicted error was within 10%. Rishbood et al. [2003] found that using neural network, surface finish could be predicted within a reasonable degree of accuracy by taking the acceleration of radial vibration of tool holder as a feedback. They suggested that any adaptive control strategy should be based preferably on soft computing techniques to account for uncertainties and imprecision.

Lo [2003] used adaptive neuro-fuzzy inference system (ANFIS) to predict the surface roughness in end milling process. The independent parameters for the cutting were spindle speed, feed rate, and depth of cut. The ANFIS model was done using triangular and trapezoidal membership functions. The average error of prediction of surface roughness for triangular membership function was found around 4%. In another study, Ho et al. [2009] applied an adaptive neural fuzzy inference system (ANFIS) with the hybrid Taguchi genetic learning algorithm to predict the surface roughness of the work-piece in the end milling process. This algorithm was used to determine the most appropriate membership functions as well as the optimal premise and consequent parameters by minimizing the root-mean-squared-error criterion.

Zain et al. [2010] applied the artificial neural network and simulated annealing techniques to determine the optimal process parameters in abrasive water jet machining operation. The input parameters used in the experiment were traverse speed, water jet pressure, standoff distance, abrasive grit size and abrasive flow rate. They investigated the quality of the cutting of machined work-piece by looking to the average roughness value (R_a). The optimal values were calculated to obtain the minimum value of R_a .

Davim and Reis [2004] studied the machinability polyetheretherketone reinforced with 30% glass fiber–PEEK GF 30 using polycrystalline diamond (PCD) and cemented carbide (K20) tools. The objectives of the study were to investigate the effects of cutting speed and feed on the cutting force, power consumption, surface roughness and international dimensional precision on the glass fiber reinforced PEEK matrix. The analysis of variance (ANOVA) was also preformed due to investigate the cutting

characteristics of PEEK GF30 using a polycrystalline diamond (PCD) and a cemented carbide (K20) cutting tool. Turning operation was performed with three levels of cutting velocities 150 m/min., 250 m/min. and 377 m/min. and three levels of feed 0.05 mm/rev., 0.10 mm/rev. and 0.20 mm/rev. According to their findings, surface roughness increased with increasing feed but decreased with increasing cutting velocity. Feed rate was found to be the parameter that influenced surface roughness most. For both the tools, cutting velocity was the parameter that had the largest influence on power, 96.9% and 96.8% for PCD and K20 respectively. The specific cutting pressure got decreased with the feed rate and increased with the cutting velocity.

Davim and Mata [2004] investigated the surface roughness of glass fiber reinforced propoxylated bisphenol after turning it with a diamond tool. The objective of their study was to determine the optimal cutting condition using multiple regression analysis (MRA). In their experiment, three levels of cutting velocities 155 m/min., 285 m/min. and 571 m/min., three levels of feeds 0.10 mm/rev., 0.20 mm/rev. and 0.30 mm/rev. were used and the depth of cut was kept constant at 0.05 mm. According to them, surface roughness of machined GFRP increased with increasing feed rate and decreased with increasing cutting velocity. Sahin and Motorcu [2005] developed a surface roughness model based on cutting speed, feed rate and depth of cut for turning of mild steel with coated carbide tools using response surface methodology (RSM). According to them, feed rate was the least influencing factor on surface roughness.

Pal and Chakraborty [2005] studied the machinability of mild steel specimen in turning it with a high speed steel cutting tool and developed a surface roughness model using artificial neural network (ANN). The input parameters for the algorithm were cutting speed, feed rate, depth of cut, feed force and cutting force. They developed a 5-5-1 network architecture where the number of input neurons was 5, the number of hidden neurons was 5 and the number of output neuron was 1. The learning rate for the program was 0.02 and momentum coefficient was assumed to be 0.90. The optimum network architecture has been found out based on the mean square error and the convergence rate. Ozcelik and Bayramoglu [2005] presented the development of a statistical model for surface roughness estimation in a high-speed flat end milling process under wet cutting conditions, using machining variables such as spindle speed, feed rate, depth of cut and

step over. First- and second-order models were developed using experimental results of a rotatable central composite design and assessed by means of various statistical tests.

Ozel and Karpat [2005] utilized neural network modeling to predict surface roughness and tool flank wear over the machining time for variety of cutting conditions in finish hard turning. Bagci and Isik [2006] investigated the surface roughness of unidirectional GFRP composites by performing turning operation. During their experiment, they varied depth of cut, feed rate and cutting speed. Throughout the operation, cutting direction was held parallel to the orientation of the fibers. Based on a three level full factorial analysis turning experiments were designed. An artificial neural network (ANN) model along with a RSM model was also developed to predict the surface roughness of the turned parts. The experimental data were put into the two developed models and found to be very accurate with a little tolerance.

Zhong et al. [2006] performed turning operation on aluminum and copper rod of diameter 19 mm to develop a surface roughness model using neural network (NN). NN was performed with seven inputs namely tool insert grade, workpiece material, tool nose radius, rake angle, depth of cut, spindle speed and feed rate. Analysis of variance approach (ANOVA) was also performed to evaluate the significance of the effects of three and four layer networks with sigmoid and hyperbolic tangent activation function. Palanikumar [2008] investigated the effect of turning on glass fiber reinforced composite using PCD tool while cutting conditions were varied. A second order surface roughness model was also developed using RSM. The reinforcing material was E glass fiber and the matrix material was epoxy resin used in the experiment. The cutting speeds were 50 m/min., 100 m/min. and 150 m/min., the feed rates were 0.10 mm/rev., 0.15 mm/rev. and 0.20 mm/rev., while the depth of cuts were 0.05 mm, 0.10 mm and 1.50 mm. Feed rate was found to be the most dominant factor influencing surface roughness followed by cutting speed. It was also found, to achieve the desired surface finish on GFRP workpiece, high cutting speed, high depth of cut and lower feeds should be preferred.

Kumunan et al. [2008] performed series of end milling operations with varying cutting speed, feed, depth of cut and vibration. Their work proposed two different hybrid intelligent techniques namely ANFIS and radial basis function neural network- fuzzy logic (RBFNN-FL) for predicting surface roughness during end milling. An experimental data

set was obtained with speed, feed, depth of cut and vibration as input parameters and surface roughness as response variable. The input-output data set was used for training and validation of the proposed techniques. After being validated, those techniques were forwarded in order to predict surface roughness. Both the hybrid techniques were found superior over their respective individual intelligent techniques when computational speed and accuracy were in concern predicting surface roughness.

Sharma et al. [2008] investigated surface roughness of adamite and measured various forces along with developing an artificial neural network (ANN) model during turning operation. Cutting speed, feed, depth of cut and approaching angle were set as the input parameters whereas feed force, thrust force, passive force and surface roughness were the chosen as the output parameters. The ANN model contained four input neurons and four output neurons. After performing the machining operation, it was found that cutting force (F_c) showed an increasing trend with the increase in approaching angle, feed and depth of cut whereas it showed a decreasing trend with speed. Passive force (F_p) increased with increase in depth of cut, speed and feed whereas it showed a decreasing trend with increase in approaching angle. The depth of cut exhibited maximum influence on passive force (F_p) in comparison to other machining parameters. Feed force (F_f) showed increasing trend with all variables i.e. approaching angle, speed, feed and depth of cut. The depth of cut exhibited maximum influence on the feed force (F_f). Surface roughness (R_a) found to be positively influenced with feed and showed a negative trend with approaching angle, speed and depth of cut. The developed neural network model could predict R_a with moderate accuracy but the model was able to predict the above mentioned three forces with high accuracy.

Shahabi and Ratnam [2010] performed turning operation on AISI stainless steel of a work material of diameter 70 mm using uncoated carbide tool. Machine vision approach was used to predict the surface roughness while the cutting condition was varied. Three levels of cutting speed 170 m/min., 188 m/min. and 206 m/min., three levels of feed rates 0.20 mm/rev., 0.25 mm/rev. and 0.30 mm/rev. and three levels of depth of cut 0.15 mm, 0.20 mm and 0.25 mm were used during the experiment. The mathematical models developed were proven to be successful to predict the average roughness and dimensional deviation at any randomized cutting conditions.

Escalona and Maropoulos [2010] performed face milling operation on Al alloy 7075-T7351 and developed a surface roughness model using artificial neural network (ANN). The radial base neural network (RBNN), feed forward neural network (FFNN), and generalized regression neural networks (GRNN) were selected for modeling surface roughness. For those, five inputs namely cutting speed, feed per tooth, depth of cut, chip width, and chip thickness were considered regardless RBNN, FFNN and GRNN. The cutting speeds selected for the experiment were 600 m/min, 800 m/min and 1000 m/min, feed rates were 0.10 mm/tooth, 0.2 mm/tooth and 0.3 mm/tooth and the selected depth of cuts were 3.0 mm, 3.5 mm and 4 mm. Based on the mean square error percentage result, it was found that feed forward network produced the best result.

Kok [2011] investigated the machinability of metal matrix composite (MMC) while performing turning operation on the workpiece. The length and the diameter of the workpiece were 140 mm and 40 mm respectively. The reinforcing material was Al_2O_3 particle whereas the matrix material was 2024 Al. The volume fraction of the reinforcing material was 7.3% and 23.3%. The cutting tools used during the experiment were titanium nitride (TiN) coated K10 carbide tool and trip layer coated P30 carbide grade (TP30). The cutting speeds used in the experiment were 100 m/min. and 210 m/min., while the feed rate and depth of cut were kept constant at 0.1 mm/rev and 2 mm respectively. A second order surface roughness model was also developed using RSM. They concluded that, the surface roughness value of the K10 tool was higher than that of the TP30 tool. The surface roughness increased with increasing cutting speed while it decreased with increasing the size and volume fraction of particles for both tools regardless of cutting conditions. Also the dependency of the surface roughness on the cutting speed was smaller when the particle size was smaller. It was also observed that the cutting speed (35.44%) was the most significant factor that had the greatest physical as well as statistical influence on the surface roughness followed by the size and volume fraction of Al_2O_3 particles (13.38% and 12.35%) for TP30 cutting tool. However in the case of K10 tool, the volume fraction of particle (51.46%) was found to be the most effective factor followed by the interaction of the particle size.

Natarajan et al. [2011] turned a workpiece made of brass of diameter 20 mm and length 85 mm with varying cutting conditions. The objective of the experiment was to

develop a surface roughness model using artificial neural network (ANN). The constructed ANN was of feed forward type and the used algorithm was back propagation of errors. Six levels of cutting speed, six levels of feeds and six levels of depth of cuts were used in the experiment. For each parameter three values were chosen to train the algorithm where the rest three were used to test the algorithm. It was found that among the individual parameters, feed rate was the most influencing parameter to affect surface roughness followed by spindle speed and depth of cut. It was also seen that the depth of cut influenced the surface roughness considerably for a given feed rate. The developed ANN model proved to be very effective in the case of predicting surface roughness.

Raju et al. [2011] performed end milling operation on 6061 Al alloy with HSS and carbide end mill cutter under both dry and wet condition. The objective of their research was to develop a second order mathematical model of surface roughness using multiple regression analysis (MRA) based on the results of ANOVA. Three levels of cutting speeds 500 rpm, 1000 rpm and 1500 rpm, three levels of feed rates 200 mm/min, 300 mm/min and 400 mm/min and three levels of depth of cuts 0.5 mm, 1.0 mm, 1.5 mm were used in the experiment. According to their findings, feed rate was a dominant parameter and surface roughness increased rapidly with the increase in feed rate and decreased with the increase in spindle speed, while the effect of depth of cut was not very regular. Surface roughness was found to decrease with the use of carbide tool in comparison to HSS tool. It was also observed that surface roughness decreased with the use of coolant. Genetic algorithm (GA) had been used to estimate the optimum machining conditions to produce the best possible surface quality abiding all the constraints. Optimum cutting condition for response variable was also tested to confirm the theoretical results and it showed fairly good agreement with values obtained from GA.

Azmi et al. [2012] studied the end milling of GFRP composite where Taguchi orthogonal array coupled with the Grey relational analysis was used to achieve optimum machinability characteristics. The material used for the experiment was 16 layers of uni-directional E-glass fibers as the reinforcement while epoxy resins as the matrix material. Three different depths, three different feed rates and three different spindle speeds were chosen for the experiment. The objectives of the experiments were to optimize the machining force, surface roughness and tool life. According to the results suggested by

Grey and statistical analysis, feed rate was the main governing factor which affected multiple machinability characteristics. Again, the optimum values of the selected parameters produced minimum surface roughness along with minimum cutting force and maximum tool life. Asilturk [2012] performed turning operation on AISI 1040 steel of hardness 35 HRC having a diameter of 100 mm and length 500 mm. The objective of the experiment was to develop a surface roughness model using neural networking and multiple regression analysis (MRA). The selected parameters were cutting speed, feed, depth of cut and nose radius of the cutting tool. The cutting speeds were 150 m/min., 219 m/min., 320 m/min., the feeds were 0.12 mm/rev, 0.20 mm/rev, 0.35 mm/rev.; the chosen depth of cuts were 1 mm, 2 mm and 4 mm. The developed predictive models found to be successful in predicting surface roughness but ANN results favored over MRA. In affecting surface roughness, feed rate was the most dominant factor followed by depth of cut and cutting speed.

Gill et al. [2013] performed machining operation in unidirectional glass fiber reinforced epoxy composite. Turning operation was done on a workpiece of diameter 42 mm and length 840 mm in both dry and wet environment. Weight percentage of fiber was kept 25 ± 5 . The cutting tool used in the experiment was carbide insert (K10). The objective of the experiment was to predict cutting force while cutting speed, feed rate, tool nose radius and tool rake angle were varied during the whole operation. Three levels of cutting speeds, three levels of feed rates, two nose radii and three different rake angles were used in the experiment. Multiple regression analysis (MRA) was used to predict the cutting force. It was found that depth of cut was the major parameter that can be attributed to high cutting force. It was also found that the tangential, feed and radial force decreased with decrease in tool nose radius. The tangential, feed and radial force increased with decrease in tool rake angle. Multiple regression analysis also proved very successful in predicting all kinds of forces.

Shahrajabian and Farahnakian [2013] performed drilling operation on CFRP with varying spindle speed, feed rate and point angle of the twist drillbit. The spindle speeds used in the experiment were 1250 rpm, 2625 rpm and 4000 rpm; while feed rates were 50 mm/min, 425 mm/min and 800 mm/min and point angles were 60° , 10° and 140° . The objective of the experiment was to determine optimal cutting parameters keeping surface

roughness, thrust force and delamination constrained up to certain level. Response surface methodology (RSM) has been used coupled with genetic algorithm to determine the optimal condition. According to their findings, The minimum surface roughness ($R_a = 0.685 \mu\text{m}$) was achieved at spindle speed of 4000 rpm, feed rate of 50 mm/min, tool angle point of 140° and the maximum surface roughness ($R_a = 2.542 \mu\text{m}$) was achieved at spindle speed of 1250 rpm, feed rate of 800 mm/min, point angle of 100° . The minimum delamination ($F_d = 1.02$) was achieved at spindle speed of 4000 rpm, feed rate of 50 mm/min, point angle of 100° , and the maximum delamination ($F_d = 2$) was achieved at spindle speed of 1250 rpm, feed rate of 800 mm/min, point angle of 140° . The developed RSM model was also successful to predict surface roughness, thrust force and delamination. By performing ANOVA, it was also confirmed that feed rate was the most dominant factor that could influence surface roughness, thrust force and delamination.

Kumar et al. [2013] performed turning operation in glass fiber reinforced plastic using carbide (10) cutting tool and presented utility concept for multi response optimization. The process parameters selected for the study were tool nose radius, tool rake angle, feed rate, cutting speed, depth of cut, and cutting environment. The objective of their study was to find statistically significant parameters to minimize surface roughness and maximize the material removal rate simultaneously. The multiple performance characteristics were surface roughness and MRR. The cutting speeds used in the experiment were 55.42 m/min, 110.84 m/min and 159.66 m/min, the feed rates were 0.05 mm/rev, 0.10 mm/rev and 0.15 mm/rev, chosen depth of cuts were 0.2 mm, 0.8 mm and 1.4 mm and the cutting environments were dry, wet and cooled. They found that the developed model based on the Taguchi approach and the utility concept was effective to achieve good performance characteristics. The depth of cut, cutting speed, and feed rate had a significant effect on the utility function based on the ANOVA significant process parameters for multiple performances. The optimal condition was determined as cutting speed 110.84 m/min, feed rate 0.1 mm/rev and the depth of cut was 1 mm.

Sreenivasulu [2013] studied surface damage and delamination of GFRP during end milling. Taguchi design method and artificial neural network (ANN) were used to determine the value of the damages. The work material used for the work was glass fiber reinforced polymeric composite material fabricated by hand layup method of 33% fiber

and 66% general purpose resin with randomly oriented long fibers supplied by Saint Gobain Vetrotex India Limited. The dimensions of the work piece were 300 mm×50 mm ×25 mm. In their study, the experiments were carried out on a CNC vertical machining center (KENT and ND Co. Ltd, Taiwan make) to perform 10 mm slots on GFRP work piece by K10 carbide, four flute end milling cutter. In addition to that, spindle speed (rpm), the feed rate (mm/min) and depth of cut (mm) were varied during experiment. Each experiment was conducted three times with spindle speeds of 1000 rpm, 1250 rpm and 1500 rpm. Feed rates were 200 mm/min, 300 mm/min and 400 mm/min and depth of cuts were 0.5 mm, 1 mm and 1.5 mm. After completing series of experiments, it was found that the primary machining characteristics such as surface roughness and delamination damage factor were studied for End milling. From S/N Ratio response graph, the combination of the values of speed 1000 rpm, feed 200 mm/min and depth of cut 1.5 mm were found to be the optimum value for surface roughness and delamination damage. From S/N Ratio response table, depth of cut, feed rate and cutting speed are the order of influence of parameters on surface roughness and delamination damage during machining of GFRP. The result of ANOVA for surface roughness suggested that depth of cut was the most significant parameter for affecting the surface roughness and cutting speed was the most significant parameter for affecting the delamination damage.

Subramanian et al. [2014] worked with Al7075-T6 material to develop a surface roughness model during end milling using RSM where the cutting tool was of high speed steel (HSS). The variables used in the experiment were cutting tool geometry and cutting condition. The cutting speeds were 75 m/min., 95 m/min., 115 m/min., 135 m/min. and 155m/min., the feeds were 0.02 mm/tooth, 0.03 mm/tooth, 0.04 mm/tooth, 0.05 mm/tooth and 0.06 mm/tooth and the used depth of cuts were 1.5 mm, 2 mm, 2.5 mm, 3 mm and 3.5 mm. According to their findings, Surface roughness increased with increasing cutting feed rate and the surface roughness increased with the decrease in cutting speed. The least increase in surface roughness was found at low nose radius, while a decrease in surface roughness was noticed at high nose radius. The surface roughness increased at low radial rake angle and surface roughness decreased at high radial rake angle. The optimal cutting parameters for the minimal surface roughness are $\gamma = 12^\circ$, $R = 0.8$ mm, $V_c = 115$ m/min, $f_z = 0.04$ mm/tooth and $a_p = 2$ mm. It was also possible to predict the surface roughness of the work material according to the developed second order surface model.

1.3 Summary of the Review

The summary of the review presents that manufacturing fraternity is constantly looking for machining products of metals and FRP composite materials without compromising quality. Machining of steels of different hardness as well as FRP composite materials has become very popular to give products the desired size and shape. Various machining environments have also been flourished in doing so. Compressed air cooling is one of those. It has gained attention due to its no harmful effect on the environment as well as it has reduced machining cost that would occur if conventional flood cooling was used. Again, where high pressure cooling (HPC), minimum quantity lubrication (MQL) fail to machine FRP materials while keeping mechanical properties of the work specimen's intact, compressed air cooling can be easily adopted since mechanical properties of FRP is retained. Different cutting condition i.e. cutting speed, feed and depth of cut are used by the researchers to find the optimal machining condition.

FRP Composite materials are being readily used in different hardcore industries due to their light weight, high specific strength and high specific modulus. They are almost manufactured in near net shape but their machining often becomes very necessary for the final finishing of the products. This reason has led the engineers to machine them with desired accuracy and precision. Their anisotropic property often poses threat to their cutting but different techniques are arriving to machine them properly. Sometimes, multiple numbers of fibers can be used to reinforce the same matrix, that FRP composite is called hybrid composite.

As an important parameter to indicate surface quality, surface roughness has already been recognized across the globe. Machined property of FRP and their surface roughness have become a matter of research interests to the researchers worldwide. Because of the dearth in resources, it may be very difficult sometimes to machine a material and that's why simulation regarding machined surface have also caught researcher's attention. Different techniques such as ANFIS, genetic algorithm (GA), MRA are getting used in the purpose of modeling of surface roughness of FRP composite.

1.4 Objectives of the Present Work

The objectives of the present work are-

- (i) Development of a hybrid composite material consisting two different fibers namely Kevlar and glass fiber. Polyester resin will be used as the matrix material for the developed composite.
- (ii) Systematic experimental study on the effects of compressed cooled air jet on the machinability characteristics of hybrid composite at different cutting velocities and feeds in terms of cutting forces and surface roughness.
- (iii) Develop a model for surface roughness using artificial neural network (ANN) while turning hybrid composite by TiN coated carbide insert under compressed air cooling condition from the characterization of the physical processes taking place during machining and its validation.

1.5 Scope of the Thesis

The growing demand of composite materials and their attractive features are driving the engineers and manufacturers constantly to work more and more on them. Development of composite material has become a matter of great deal to the material engineers and researchers throughout the world. Again, the characterization of FRP composites machinability is becoming a research interest as they often need to be machined to produce the desired shape and size. This thesis contains several chapters.

Chapter 1 presents the main aims and objectives of machining operation, works that have been previously done on FRP composites keeping their mechanical properties on thoughts, complications associated with machining a FRP material, the main reasons of compressed air cooled machining being popular these days as well as the techniques that are used to model surface roughness of a machined surface. This chapter also provides the main goals of this research.

Chapter 2 presents the development of the hybrid composite material where two different fibers i.e. Kevlar and glass fiber have been used to reinforce the same matrix material. In this research work, polyester has been used as the matrix material.

Chapter 3 deals with the machining investigation and experimental findings that have been attained by performing turning operation on the developed hybrid composite material under both dry and compressed air cooling condition. It also presents the graphical representations that show variation of average surface roughness and main cutting force with different cutting condition under both machining environments.

Chapter 4 explains the theory, structure, learning paradigm and also error minimization technique of artificial neural network (ANN). Again, the chapter also presents the modeling of surface roughness of the developed hybrid composite turned under compressed air cooling condition. The chapter concludes with the validation of the developed ANN model for predicting surface roughness.

Chapter 5 contains the detailed discussions on the experimental results regarding the machined surface roughness, main cutting force and artificial neural network model for predicting surface roughness. Again, possible interpretations of the results are presented in this chapter. The reduction of main cutting force and surface roughness due to the usage of compressed air cooling are also presented in tabulated form. This chapter also contains the discussion regarding the modeling of surface roughness of Kevlar and glass reinforced polyester. Finally, a summary of major contributions, recommendation for the future work and references are provided at the end.

Chapter-2

Material Development

2.1 Introduction

Major constituents in a FRP composite are fiber and the matrix. The matrix acts as a binder for the reinforcing agents. Similar to that, in a hybrid composite material also, fibers and the matrix are the main components. By impregnating two or more types of fibers in the same matrix, hybrid composites are formed. One fiber may be of low elongation (LE) and the other one may be of high elongation (HE). Hybrid composites provide a large range of mechanical properties and the cost of the material can be greatly reduced by keeping them reasonably good for services. However, to predict the mechanical properties of a hybrid composite the rule of mixture (ROM) may not work very well. They often show ‘_hybrid effect’ which is defined as the difference between the failure strain of the LE fiber in a hybrid composite and that in a pure LE fiber composite. A positive hybrid effect is identified when the value of the property is above that of achieved by ROM while negative hybrid effect means the value of the property is lower than the ROM value. The hybrid effect has been thought to be caused by (i) thermal residual stress and (ii) smaller dynamic stress concentration factors. [Yiping and Schwartz 1992].

2.2 Development of Hybrid Composite Material

The function of the fibers in a composite is extremely important since they are responsible for carrying the significant percentage of the applied load. Keeping this in thought; in this research, two different fibers namely Kevlar and glass fiber have been used as the reinforcing material for the developed hybrid composite. Kevlar fiber belongs to a group of highly crystalline aramid fibers. Researchers have suggested that it is an aromatic polyamide which is chemically known as ‘_poly paraphenylene terephthalamide’. They have become very popular for having highest specific modulus and highest specific

strength. They have found their applications in marine and aerospace. Kevlar fiber has mean tensile strength of 2.75 GNm^{-2} and it has a modulus of 120 GNm^{-2} along with a density of 1.45 gcm^{-3} . These properties have made it an attractive fiber to reinforce polymers. For a mean fiber content of 53.2%, the Kevlar 49 composite yielded a compressive strength of 227 MNm^{-2} . [Greenwood and Rose 1974]. Kevlar fibers are also getting heavily used in cryogenics because of their low thermal conductivities and high values of both tensile strengths and modulus of elasticity [Ventura and Martelli 2009]. But the main weakness of Kevlar is their very low compressive strength as well as they have a very poor machining property.

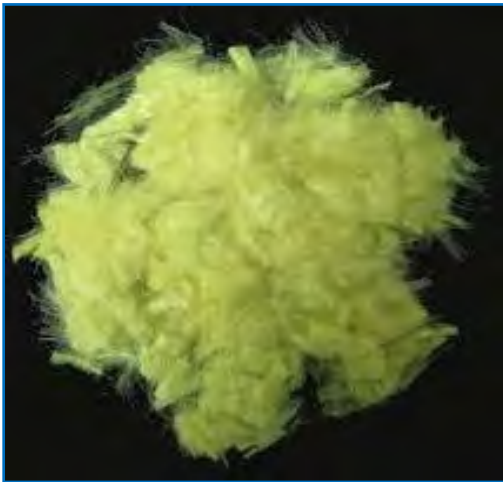


Fig. 2.1: Kevlar fiber in fibrous form

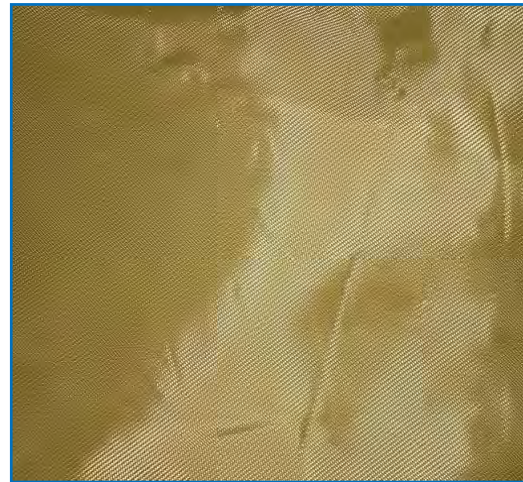


Fig. 2.2: Kevlar fiber in the form of fabric



Fig. 2.3: Glass fiber in two different forms

Glass fibers are the most common of all reinforcing fibers. As opposed to Kevlar, they are inorganic and non crystalline fibers. They are preferred for their low cost, high tensile strength, excellent insulating properties and good machinability as well. But their limitations lie in their high specific gravity, high hardness which may cause wears to the

cutting tools. Their compressive strength is much better than Kevlar. In comparison to Kevlar's compressive strength of 227 MNm^{-2} , a glass composite with a volume fraction of 50% gave a compressive strength value of 456 MNm^{-2} .

The main role of the matrix in a FRP composite is acting as a binder for the fibers but it also has some other important tasks to accomplish i.e. (i) transferring stresses between the fibers, (ii) providing a barrier against an adverse environment and (iii) to protect the surface of the fibers from mechanical abrasion. In general, both the strength and the stiffness of the matrix are much lower than the fiber's. The matrix is more of ductile nature and since the Young's modulus of matrix is considerably lower than that of fiber, the matrix carries only a small portion of the total load. So, a composite where the failure is strain dominant, it is presumed that no damage would take place in matrix during loading. As adhesion between the fiber and matrix improves the efficiency of load transfer also increases. In this thesis polyester has been chosen as the matrix material. Polyester is one kind of thermoset materials that has found its applications as a matrix material in automotive and aerospace. The properties of this resin depends on its cross linking density. It has a few disadvantages but its advantages are low cost, low viscosity and fast curing time. Its high volumetric shrinkage also allows the part to be released easily from the mold. Keeping these advantages in thoughts, polyester has been selected as the matrix material for the developed hybrid composite.

A cylindrical bar of hybrid composite material was developed by casting the raw materials i.e. Kevlar, glass fiber and polyester together in a cylindrical mold. The developed work material is shown in Fig. 2.4.



Fig. 2.4 Work material (Kevlar and glass fiber reinforced polyester)

Chapter-3

Experimental Investigations

3.1 Experimental Procedure and Conditions

In contrary to steels, composite materials are inhomogeneous and anisotropic in nature. Their behaviors depend upon factors such as the fiber and matrix properties, orientation of the fibers, bond strength between the fibers and the matrix and on the type of weave. Taking these factors into consideration, in order to characterize the machinability property of the developed work material, turning operation was done on the workpiece using different combinations cutting speed, feed, depth of cut along with varying machining environments which were dry and compressed air cooling condition.

It is quite established that in comparison to dry cutting, compressed air cooling has a number of advantages in the case of cutting steels but in the case of cutting a composite material this established truth may or may not hold true. The differences of physical, chemical and mechanical properties between steels and composite materials have led us to perform machining investigation on the developed hybrid composite material. The machine tool used during the machining investigation was KL-3280C/2000 (Sunlike Engine Lathe). The specifications of the machine tools were- 50 Hz, 1440 rev. /min., 7.5 kW, 420 V and 13.9 A. During the experimentation; 4 levels of cutting speeds specifically 74 m/min., 106 m/min., 149 m/min. and 213 m/min., 4 levels of feeds specifically 0.10 mm/rev., 0.12 mm/rev., 0.14 mm/rev. and 0.16 mm/rev. and 3 levels of depth of cuts 1.0 mm, 1.5 mm and 2.0 mm were used to assess the machinability of developed composite material. So according to the experimental design, for each of the dry and compressed air cooling machining environment, 48 ($4 \times 4 \times 3$) combinations of average surface roughness and cutting force were found where each machining response i.e. main cutting force and surface roughness resulted from a particular set of data containing cutting speed, feed and depth of cut. Combining both the environments, a total of 96 combinations were found after conducting the whole machining investigation. The main purpose of carrying out

machining investigation is to observe the impact of cutting speed, feed and depth of cut on the main cutting force and surface roughness of the machined part for both dry and compressed air cooling environment. The cutting conditions and process parameters of the experimental investigation are listed on the Table 3.1.

After a vigorous study on machining of fiber reinforced plastic (FRP) material, it was found that both coated and uncoated carbide have been used previously to machine FRP material along with single crystalline diamond (SCD), polycrystalline diamond (PCD) and cubic boron nitride (CBN) tool. Again, it was also found that the coated carbide insert performed much better than uncoated carbide whereas PCD tool outperformed SCD and CBN tools based on the manufactured product quality. Another important thing to remember is high speed steel (HSS) cutting tool should not be used in machining composites as they have a very low wear resistance. So, to facilitate the research smoothly and keeping product quality and cost in concern, titanium nitride (TiN) coated tungsten carbide (WC) has been chosen as the tool material for machining Kevlar- glass reinforced polyester composite under both dry and compressed air cooling condition. Fig. 3.1 shows the photographic view of the experimental setup. Another important thing to remember is the accuracy of the whole compressed cooling process depends on the delivery of cooled air in the chip- tool and work- tool interface. The nozzle position owing to deliver cooled air onto the chip- tool interface is shown in Fig. 3.1. Table 3.1 presents the experimental conditions for the machining investigation.

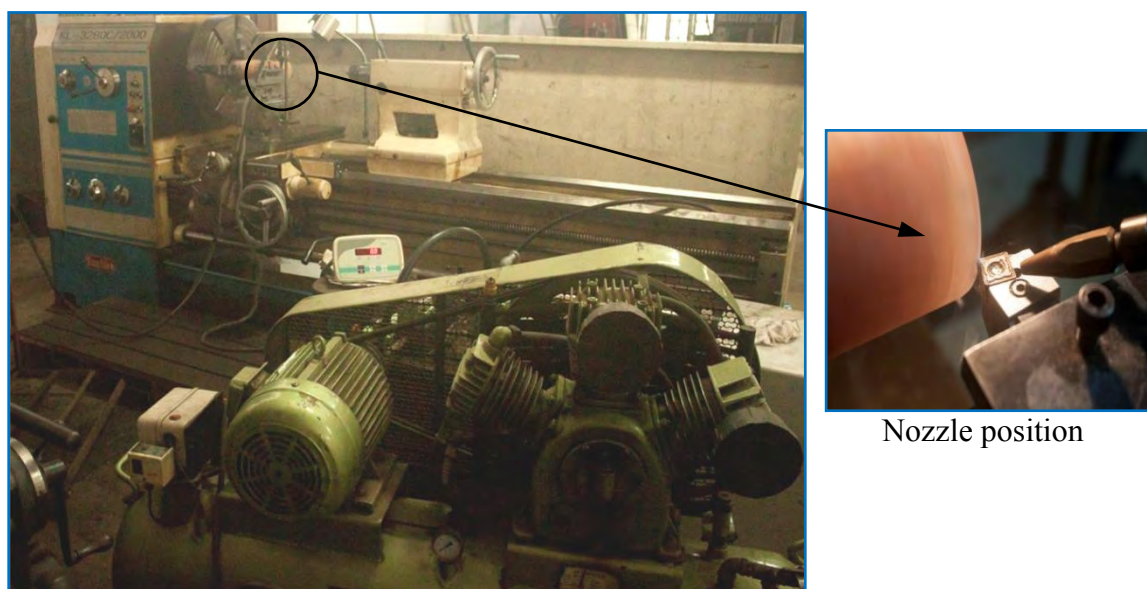


Fig. 3.1 Photographic view of the experimental setup

Table 3.1: Experimental conditions

Machine Tool	: KL-3280C/2000 (Sunlike Engine Lathe, 7.5 kW).
Work Material	: Kevlar and glass reinforced Polyester
Dimension	: 300 mm length and 100 mm diameter.
Cutting Insert	: Titanium nitride coated tungsten carbide (SNMG)
Cutting Tool Geometry	: -6°, -6°, 6°, 6°, 15°, 75°, 0.8 (mm)
Process Parameters	
Cutting Speed, V_c	: 74, 106, 149 and 213 (m/min)
Feed, S_o	: 0.10, 0.12, 0.14 and 0.16 (mm/rev.)
Depth of cut, t	: 1.0, 1.5 and 2.0 (mm)
Machining Environment	: Dry and Compressed air cooling (Air pressure- 20 Bar)

3.2 Experimental Results

After conducting a series of straight turning operations on the developed cylindrical hybrid composite bar using 4 levels of cutting speeds, 4 levels of feeds and 3 levels of depth of cuts under both dry and compressed air cooling condition; 96 combinations of surface roughness and main cutting force were found. The characterization of the machinability of hybrid composite was performed by measuring the machining response main cutting force and surface roughness of the machined part.

During the experiment the main cutting force was measured by a strain gauge dynamometer and the magnitude of the main cutting force was displayed by the charge amplifier in ‘kg’ unit. After performing the cutting operation surface roughness was measured respectively using a Talysurf (Surtronic 3+ Roughness checker, Taylor Hobson, UK) using a sampling length of 4.00 mm. The values of machining responses resulted from different cutting condition and machining environment were collected and tabulated and these values of the responses have been used to characterize the machinability property of the developed hybrid composite material.

The figures from Fig.3.2 to Fig.3.4 present the variation of main cutting force (P_z) with feed (S_o) whereas from Fig.3.5 to Fig.3.7 present the variation of main cutting force (P_z) with cutting speed (V_c) while machining FRP by coated carbide insert (SNMG) under both dry and compressed air cooling condition.

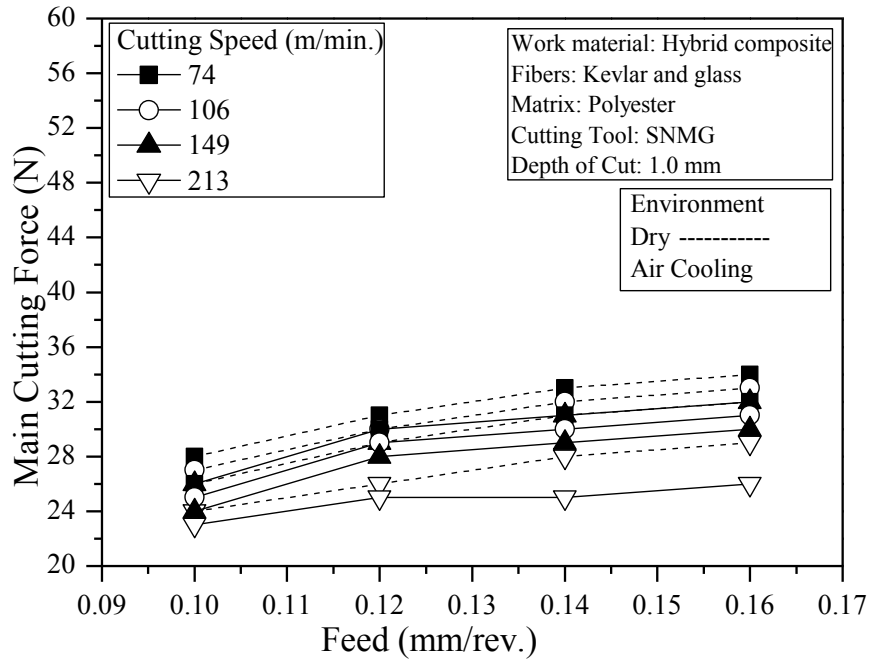


Fig. 3.2 Variation of main cutting force with S_o at different V_c and 1.0 mm depth of cut under both dry and compressed air cooling condition

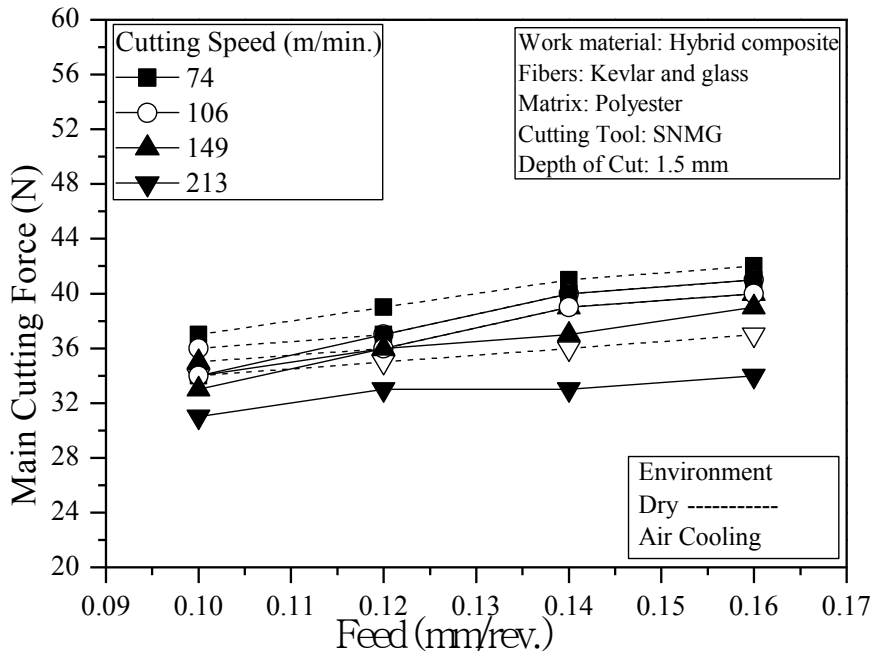


Fig. 3.3 Variation of main cutting force with S_o at different V_c and 1.5 mm depth of cut under both dry and compressed air cooling condition

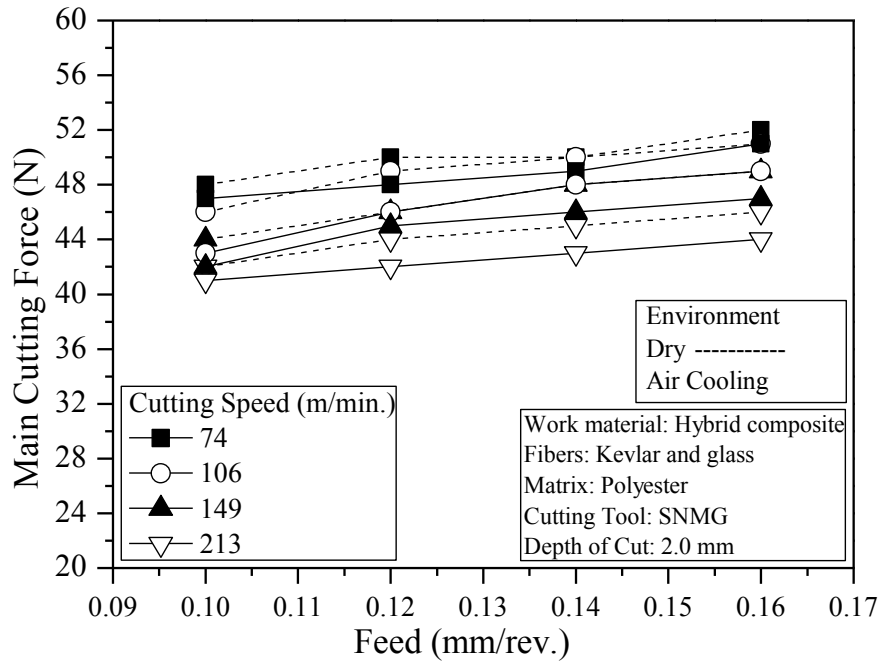


Fig. 3.4 Variation of main cutting force with S_o at different V_c and 2.0 mm depth of cut under both dry and compressed air cooling condition

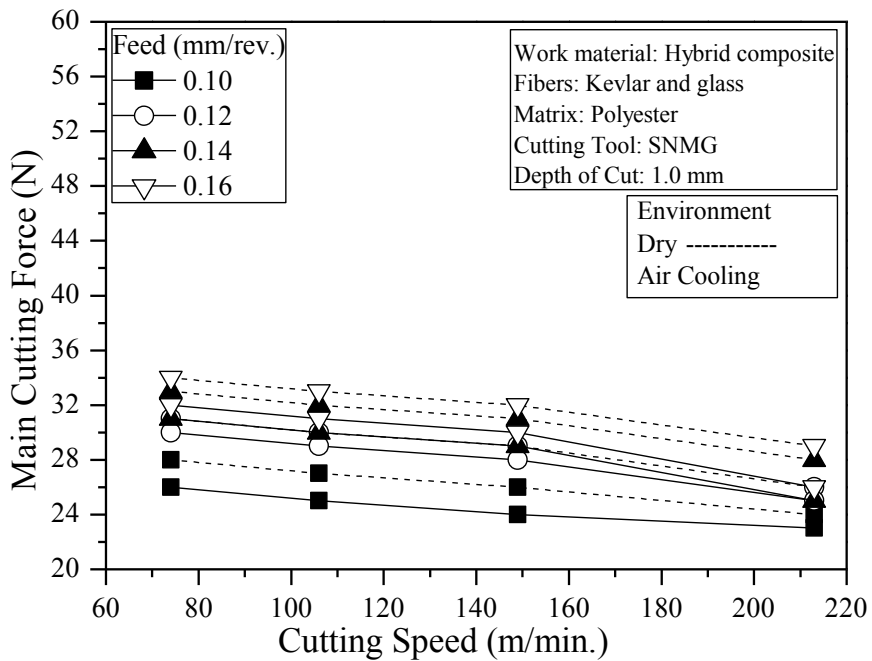


Fig. 3.5 Variation of main cutting force with V_c at different S_o and 1.0 mm depth of cut under both dry and compressed air cooling condition

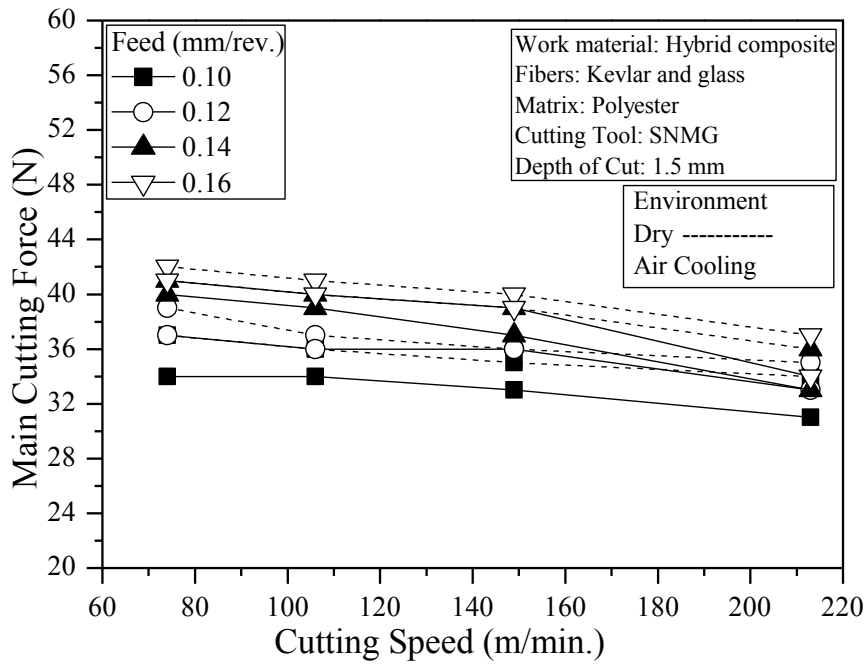


Fig. 3.6 Variation of main cutting force with V_c at different S_o and 1.5 mm depth of cut under both dry and compressed air cooling condition

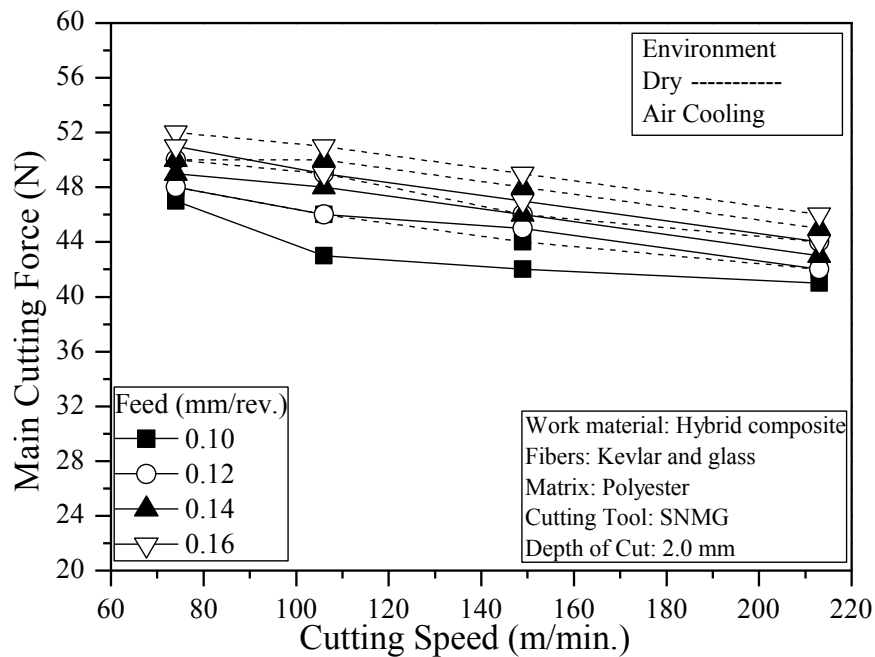


Fig. 3.7 Variation of main cutting force with V_c at different S_o and 2.0 mm depth of cut under both dry and compressed air cooling condition

The figures from Fig.3.8 to Fig.3.10 present the variation of surface roughness (R_a) with feed (S_o) whereas from Fig.3.9 to Fig.3.11 present the variation of surface roughness (R_a) with cutting speed (V_c) while machining FRP by coated carbide insert (SNMG) under both dry and compressed air cooling condition.

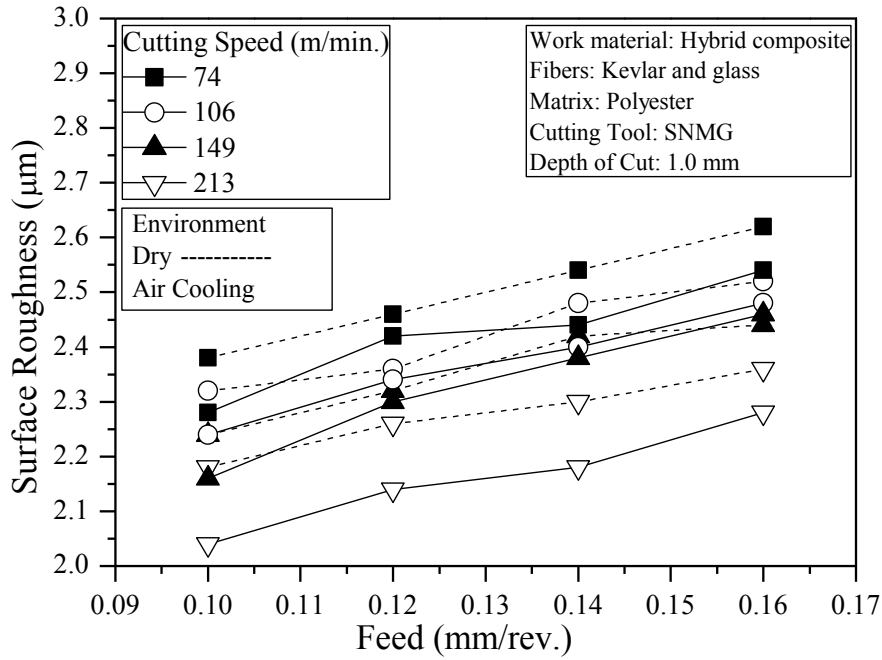


Fig. 3.8 Variation of surface roughness with S_o at different V_c and 1.0 mm depth of cut under both dry and compressed air cooling condition

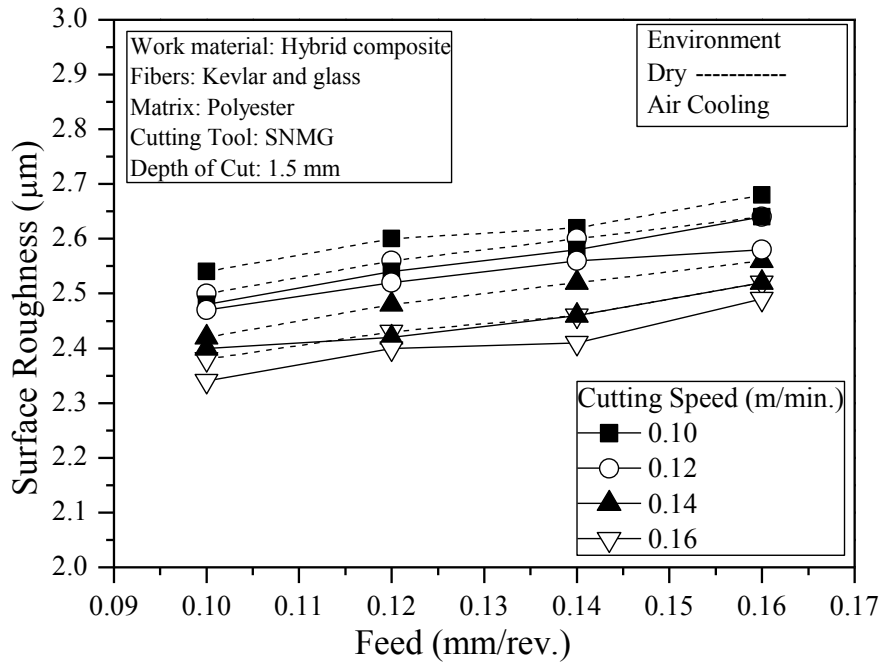


Fig. 3.9 Variation of surface roughness with S_o at different V_c and 1.5 mm depth of cut under both dry and compressed air cooling condition

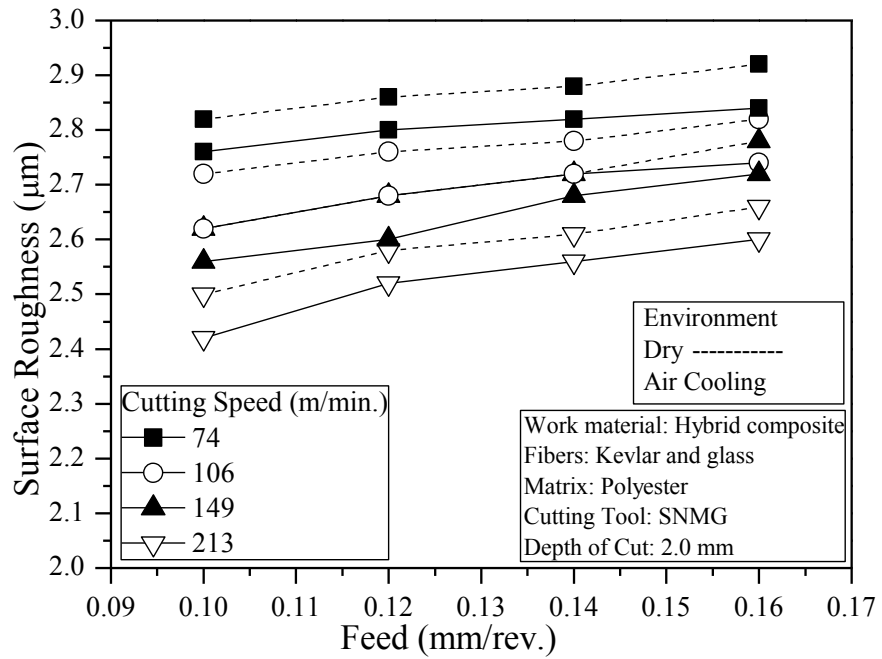


Fig. 3.10 Variation of surface roughness with S_o at different V_c and 2.0 mm depth of cut under both dry and compressed air cooling condition

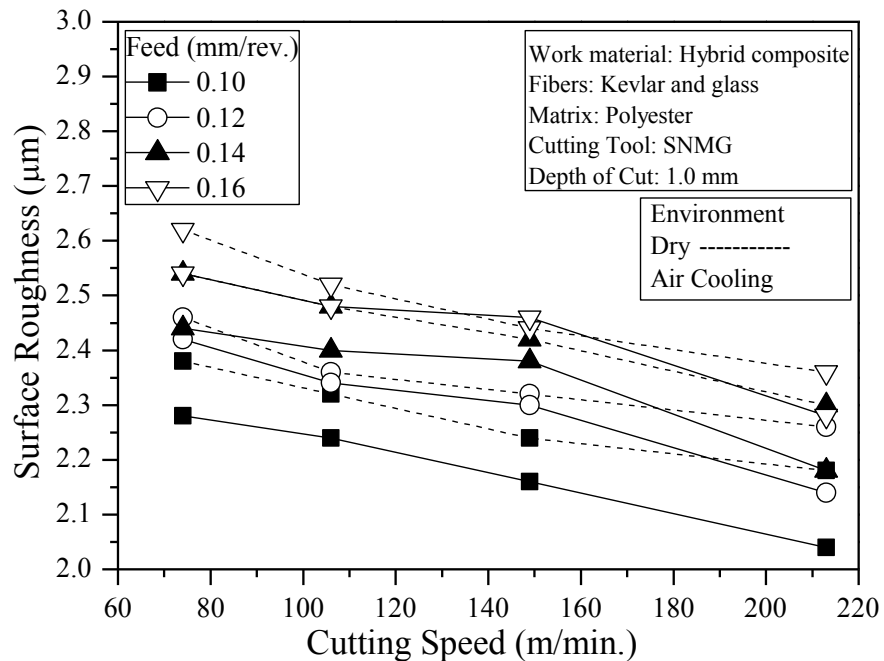


Fig. 3.11 Variation of surface roughness with V_c at different S_o and 1.0 mm depth of cut under both dry and compressed air cooling condition

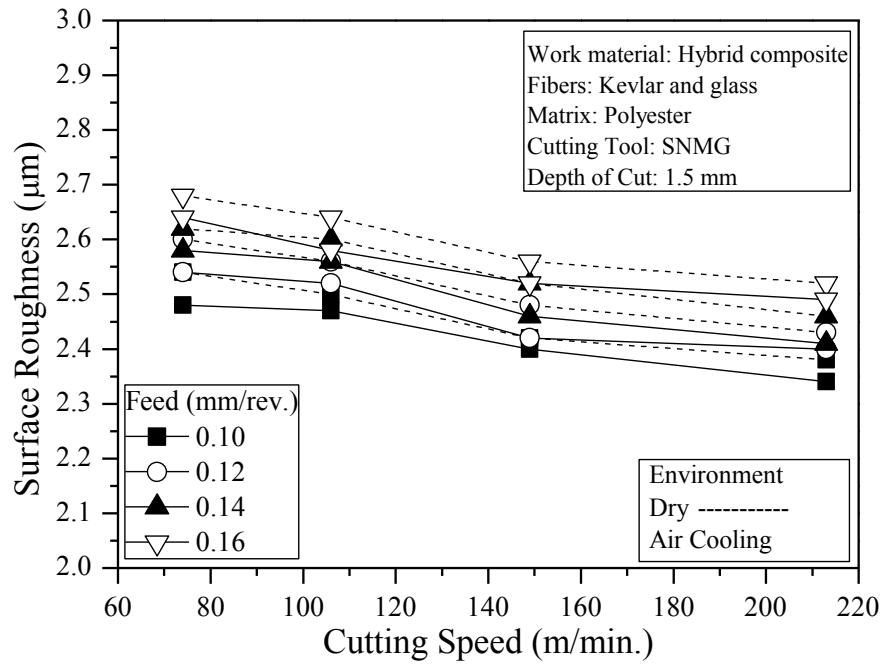


Fig. 3.12 Variation of surface roughness with V_c at different S_o and 1.5 mm depth of cut under both dry and compressed air cooling condition

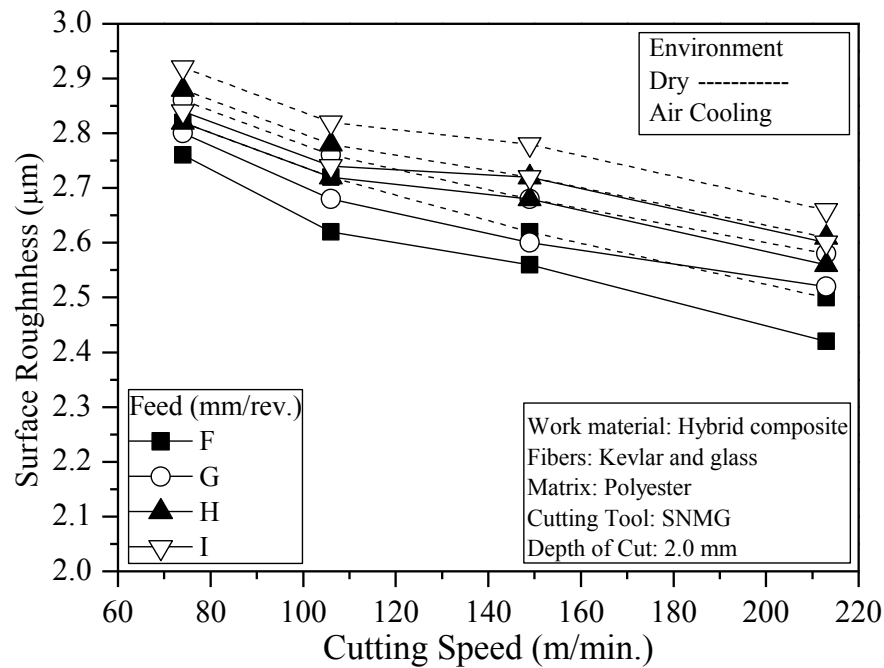


Fig. 3.13 Variation of surface roughness with V_c at different S_o and 2.0 mm depth of cut under both dry and compressed air cooling condition

Chapter-4

Modeling of Surface Roughness

4.1 Introduction

Modeling of surface roughness has become a priced technique to describe the machining environment and cutting parameters that are going to suit the material to be machined. An established model of any machining response for a particular material and a process helps the engineers to choose cutting parameters reasonably accurately which ultimately lead to the optimization of cutting condition. A great deal of research works have been carried out regarding the modeling of surface roughness for a number of materials and processes using different techniques such as response surface methodology (RSM), adaptive neuro fuzzy inference system (ANFIS), genetic algorithm (GA), radial basis neural network (RBN) etc. This thesis presents predictive model of surface roughness of Kevlar and glass fiber reinforced polyester turned under compressed air cooling condition using artificial neural network (ANN). In this model, cutting speed, feed and depth of cut have been varied to predict the average surface roughness. In order to understand the model, theory of ANN is also very necessary to be understood. Literature review regarding this area has been provided in section 1.2.4.

4.2 Artificial Neural Network (ANN)

Artificial neural network (ANN) is a powerful tool to model different kinds of problems especially those which have no authentic governing equation for their behaviors. The model obtained using ANN can learn and mimic the human thinking process [Mahdavinejad et al. 2013]. A neural network can therefore be trained to find solutions, recognize patterns, classify data and forecast future events. The behavior of a neural network is defined by the way its individual computing elements are connected and by the strengths of those connections, or weights. The weights are automatically adjusted by

training the network according to a specified learning rule until it performs the desired task correctly.

4.2.1 Structure of Neural Network

The core elements of a neural network are the neurons. Neurons are connected to each other with a set of links, called synapses and each synapse is described by a synaptic weight. Neurons are placed in layers and each layer's neurons operate in parallel. The first layer is the input layer. Non-processed information enters into input layer of the network and no computation is performed at that layer. The hidden layers follow the input layer and the activity of each hidden unit is determined from the activity of the input units and the weights at the connections of input and hidden units. A network can have many or no hidden layers and their role is to improve the network's performance. The existence of these layers at the network becomes more necessary as the number of input neurons grows. In general, there is no standard algorithm for calculating the proper number of hidden layers and neurons. For relatively simpler systems, as the present case, a trial-and-error approach is usually applied in order to determine the optimal architecture for a problem. Networks that have more than one hidden layer have the ability to perform more complicated calculations. The existence of more than necessary hidden layers complicates the network, which results in a low speed convergence during training. Therefore, the architecture of a neural network always depends upon the specific situation examined and must not be more complex than needed. The last layer is the output layer. The behavior of output units depends upon the activity of the hidden units and the weights between hidden units and output units. The output of the layer is the output of the whole network. Output layer neurons, in contrast to input layer neurons, perform calculations.

4.2.2 Types of Neural Network

There are two types of neural networks: the feed-forward types and the recurrent ones. Feed-forward neural networks allow the signals to travel in only one direction which is from input to output i.e. the output signal of a neuron is the input of the neurons of the following layer and never the opposite. The inputs of the first layer are considered the input signals of the whole network and the output of the network is the output signals of last layer's neurons. On the contrary, recurrent networks include feedback loops allowing

signals to travel forward and/or backward. Feed-forward neural networks are characterized by simple structure and easy mathematical description. Therefore, they have been selected for the modeling of surface roughness in the present thesis. Fig. 4.1 presents a feed forward neural network containing three input neurons in input layer, 1 hidden layer containing 4 neurons and an output layer containing one output neuron.

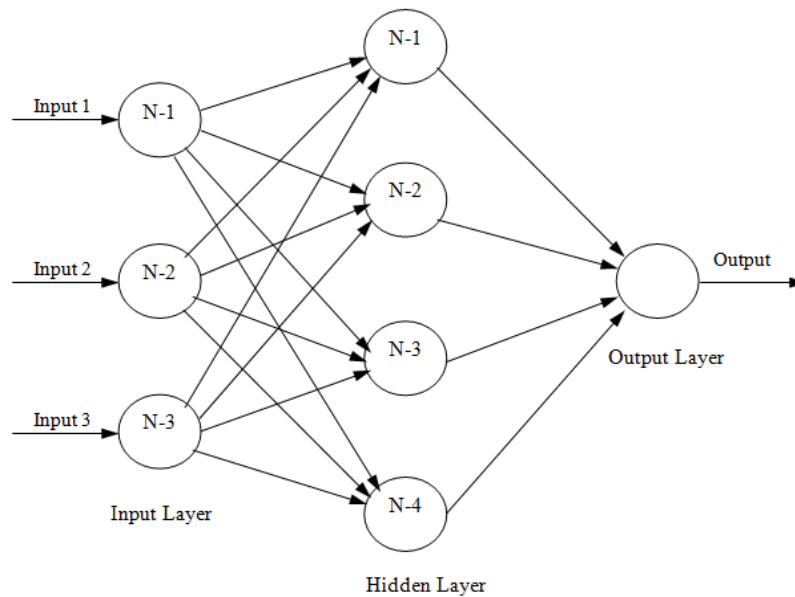


Fig. 4.1 Feed forward neural network

Multiple layers of neurons with transfer functions allow the network to learn relationships between input and output vectors. These relationships can be both linear and non linear. The linear transfer function `_puelin'` shown in Fig.4.2a is most often used for function fitting or nonlinear regression problems. According to this transfer function, the neuron's both input and output can be ranged from 0 to infinity. However, if the outputs of a network are chosen to be constrained such as between 0 and 1, then a sigmoid transfer function e.g. `logsig` (Fig.4.2b) should be used in the output layer. The function `logsig` generates outputs between 0 and 1 as the neuron's net input goes from negative to positive infinity. Alternatively, hyperbolic tangent sigmoid (Fig.4.2c) transfer function `_tansig'` can also be used in multilayer neural networks. The main difference between a `logsig` transfer function and a `tansig` transfer function is that `logsig` constrains the output value in the range of 0 to 1; whereas a `tansig` constrains the value of the output in the range of -1 to +1. Both of these transfer functions are simultaneously used for pattern recognition problems.

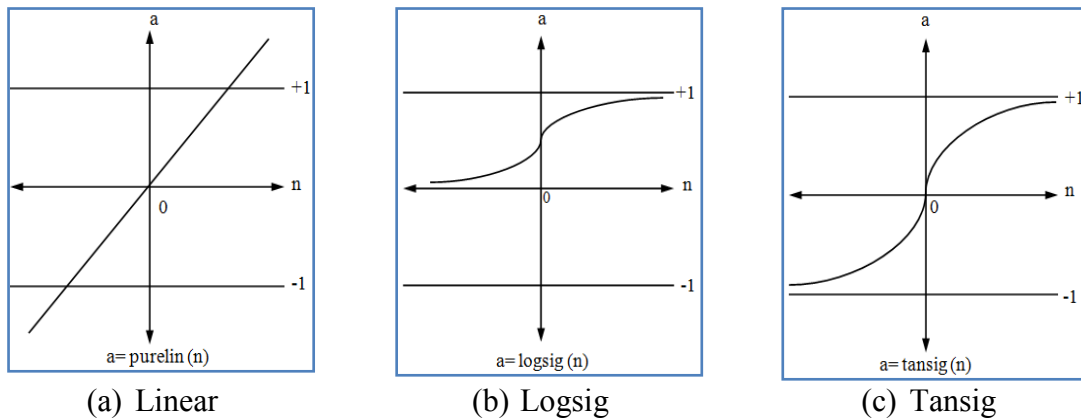


Fig. 4.2 Transfer functions

4.2.3 Learning Techniques and Error Minimization

Two learning techniques are readily used in this machine learning process. Among these two, supervised learning algorithm analyzes the training data and produces an inferred function, which can be used for mapping new examples. The training data consist of a set of training examples. In this technique, each example is a pair consisting of an input object and a desired output value. In this thesis, supervised learning paradigm has been used to predict the surface roughness for a given cutting condition.

The error of a particular configuration of the network can be determined by running all the training cases through the network and comparing the actual output generated with the desired or target outputs. The differences are combined together by an error function resulting the network's error. The procedure is repeated until mean square error (MSE) comes down to the desired level. Each time the program passes through all pairs of training vectors an epoch is completed. Usually a tentative number of epochs are provided for solving neural network problems. It is considered okay if the neural network finds a solution within the given number of epochs but if the network fails to do so within that limit of epochs, then the number of epochs is increased for getting a desirable solution.

One of the most frequently used training algorithms is the back propagation (BP) algorithm. It is usually applied in feed forward networks with one or more hidden layers. The input values vectors and the corresponding desirable output values vectors are used for the training of the network until a function is approached which relates the input vectors with the particular output vectors. When the value of the mean square error is calculated, it

is propagated to the backward direction in order to minimize the error with the appropriate modification of the weights. All of the used data in forming the network have to be in normalized form; Normalization is a method used in neural networks so that all the data present a logical correlation i.e. all input and output data are suitably transformed so that their mean value become equal to zero and the standard deviation equal to one. Otherwise, the neural network could suppose that a value is more significant than the others because of possessing a greater arithmetic value. After normalization all inputs become equally significant for the training of the network. The training algorithm used in this thesis was back propagation (BP) of errors. The last one is test group and its error is not used during training. It is used to check the validity of the model against the target values.

4.3 ANN Input and Output

Prior to develop the ANN model to predict surface roughness, the factors that affect the process performance need to be considered first:

Firstly, the machining variables which include cutting speed (V_c), feed rate (S_o) and depth of cut (t). These parameters can be set up in advance because of this reason, they are considered as controllable factors. These parameters have been used as the input parameters in the proposed ANN model.

The tool geometry consisting of nose radius, rake angle, cutting edge angle, and clearance angle can also be an important factor depending on the tool to be chosen for a particular machining process. This present machining investigation was carried out under a particular tool-work combination, which suggests tool geometry was constant. So, it has not been considered in the ANN model which was proposed as a predictive model for surface roughness.

If the used material is produced under proper quality control, the parameters indicating workpiece properties can be considered as controllable. As mentioned earlier, based on the fact that the experiment was carried out for a particular tool-work combination; that is why chemical and physical properties of machined material can be considered constant. So, it has not been considered in the ANN model which was proposed to predict tool wear and surface roughness.

Auxiliary tooling e.g. clamping system can be considered as controllable, if the clamping process is done correctly. Improper clamping can result in severe vibration therefore deteriorate the machining process and ultimately damage to the workpiece integrity. It was assumed that clamping was done properly during the machining operation and has not been considered in the proposed ANN model.

Vibrations may also occur between the workpiece and the machine tool as well as between the machine tool and the cutting tool. These factors influence the process performance to a great extent. For simplicity, undesired vibration has not been considered in the proposed neural network model.

The only one machining response that was considered as the output of neural network was surface roughness. The surface parameter used to evaluate surface roughness in this study is the average roughness average (R_a). This parameter is also known as the arithmetic mean roughness value, arithmetic average (AA), or centerline average (CLA). Within the presented research framework, the discussion of surface roughness is focused on the universally recognized. R_a is recognized universally as the commonest international parameter of roughness. The average roughness is the area between the roughness profile and its center line, or the integral of the absolute value of the roughness profile height over the evaluation length [Lela et al. 2008]. Therefore, R_a is specified by the following equation:

$$R_a = \frac{1}{L} \int_0^L |Y(x)| dx, \quad \dots\dots\dots(4.1)$$

When R_a is evaluated from digital data, the integral is normally approximated by a trapezoidal rule:

$$R_a = \frac{1}{n} \sum_{i=1}^n |Y_i| \quad \dots\dots\dots(4.2)$$

Where, R_a is the arithmetic average deviation from the mean line (μm), L is the sampling length, and Y is the ordinate of the profile curve. Graphically, the average roughness is the area between the roughness profile and its center line divided by the evaluation length. Surface roughness is a widely used index of product quality and in most cases a technical requirement for mechanical products. The performance and surface life of

any machined component is influenced by surface integrity of that component. To develop the model of surface roughness the value of average surface roughness, R_a was measured after each trial with the progress of machining.

All of the input parameters of the neural network have been kept constant throughout the modeling process except the number of neurons in hidden layer. The number of the hidden neurons has been chosen by trial and error approach. Finally, six different numbers of hidden neurons were selected for the modeling purposes and those were 20, 25, 30, 33, 35 and 40. Transfer functions have been kept constant in both of the hidden and output layer to find the optimum neural network model. The transfer function used in the hidden layer was hyperbolic tangent sigmoid ‘ tansig ’ whereas the transfer function selected for the output layer was linear transfer function ‘ puelin ’. Again, both momentum constant and learning rate of the neural network have been selected 0.5. The learning scheme used in the present work was supervised learning method whereas the selected learning rule was gradient descent rule. In all of the designed neural networks, backpropagation algorithm was used for the training purpose.

In order to find out the optimal neural network architecture, six networks with different number of hidden neurons were designed and tested. The designed networks were 3-20-1, 3-25-1, 3-30-1, 3-33-1, 3-35-1 and 3-40-1. The numbers in each of the network designate the number of inputs, number of neurons in the hidden layer and the number of neurons in output. Before training the network, the input-output dataset were normalized within the range of -1 to +1 using the Matlab command ‘ premnmx ’. The normalized value (x_i) for each raw input-output dataset (d_i) was calculated as-

$$x_i = \frac{2}{d_{\max} - d_{\min}} (d_i - d_{\min}) - 1 \quad \dots\dots\dots(4.3)$$

where,

- x_i = normalized value
- d_i = original value of input/output
- d_{\min} = minimum value of input/output
- d_{\max} = maximum value of input/output

In the present work, six neural networks have been designed, trained and tested in order to determine the optimal ANN architecture. Among the 48 combinations of R_a under compressed air cooling condition; 36 combinations have been used in the training process whereas the rest 12 combinations have been used in the testing process. Surface roughness resulted from each of the depth of cut among 1.0 mm, 1.5 mm and 2.0 mm; four cutting speeds 74 m/min., 106 m/min., 149 m/min. and 213 m/min. and three feeds 0.10 mm/rev., 0.12 mm/rev., and 0.14 mm /rev. were used for the training purpose of the neural network. In the case of testing of the neural network, surface roughness have been taken from three depth of cuts, four cutting speeds but from only one feed of 0.16 mm/rev. Table 4.2 shows the cutting conditions and the surface roughness values used in the training and the testing process. For the purpose of modeling, values of surface roughness were taken only from the machining of hybrid composite under compressed air cooling condition. Fig. 4.3 presents the schematic diagram of the developed neural network.

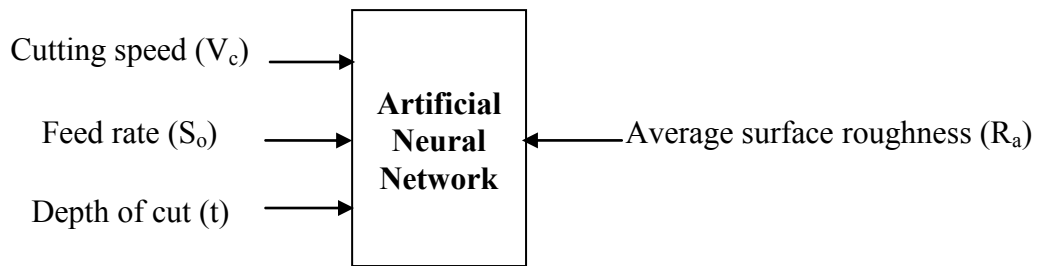


Fig. 4.3 Schematic diagram of ANN for Surface Roughness

Table 4.1 Data for training and testing

Data used in training				Data used in testing			
t (mm)	V _c (m/min)	S _o (mm/rev)	R _a (μm)	t (mm)	V _c (m/min)	S _o (mm/rev)	R _a (μm)
1.0	74	0.10	2.28	1.0	74	0.16	2.54
		0.12	2.42				
		0.14	2.44				
	106	0.10	2.24				
		0.12	2.34				
		0.14	2.40				
	149	0.10	2.16				
		0.12	2.30				
		0.14	2.38				
	213	0.10	2.04				
		0.12	2.14				
		0.14	2.18				
1.5	74	0.10	2.48	1.5	74	0.16	2.64
		0.12	2.54				
		0.14	2.58				
	106	0.10	2.47				
		0.12	2.52				
		0.14	2.56				
	149	0.10	2.40				
		0.12	2.42				
		0.14	2.46				
	213	0.10	2.34				
		0.12	2.40				
		0.14	2.41				
2.0	74	0.10	2.76	2.0	74	0.16	2.84
		0.12	2.80				
		0.14	2.82				
	106	0.10	2.62				
		0.12	2.68				
		0.14	2.72				
	149	0.10	2.56				
		0.12	2.60				
		0.14	2.68				
	213	0.10	2.42				
		0.12	2.52				
		0.14	2.56				

The performances of training of the 3-20-1, 3-25-1, 3-30-1, 3-33-1, 3-35-1 and 3-40-1 neural networks, the best fitted regression line of their training and the comparison between the experimental surface roughness value of hybrid composite turned under compressed air cooling condition and the predicted surface roughness value by ANN are presented in the figures from Fig. 4.3 to Fig. 4.8 respectively.

The ultimate goal of a model is to provide accurate and reliable forecasts about the variables of interest, in this research work which is surface roughness of the machined

part. The utilization of a model, therefore, requires the evaluation of the extent to which the model represents the underlying phenomena. This is accomplished by means of model validation. The developed ANN model has also been validated against the experimental data. The figures showing the comparison between experimental values and values predicted by ANN are the ones confirming model's validation.

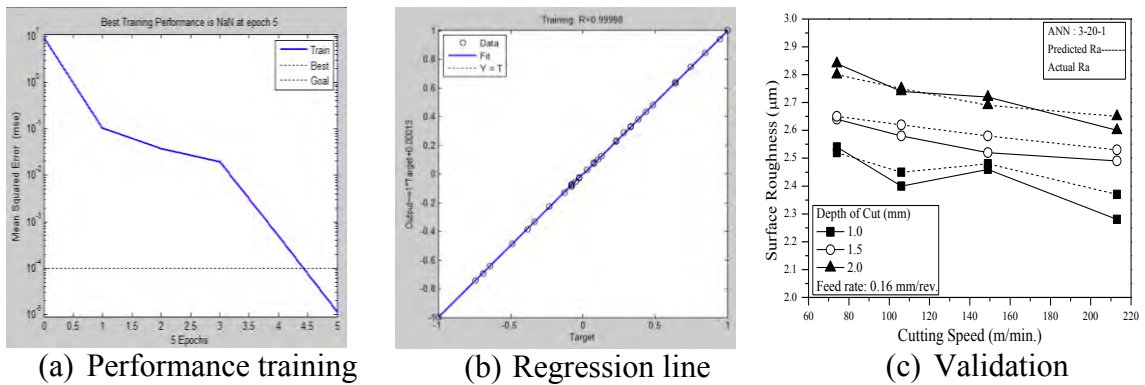


Fig. 4.4 Performance measure of 3-20-1 network

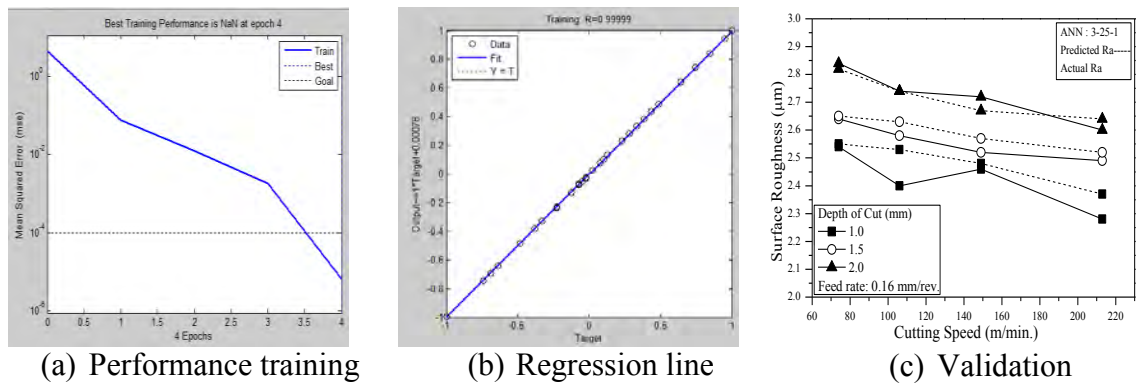


Fig. 4.5 Performance measure of 3-25-1 network

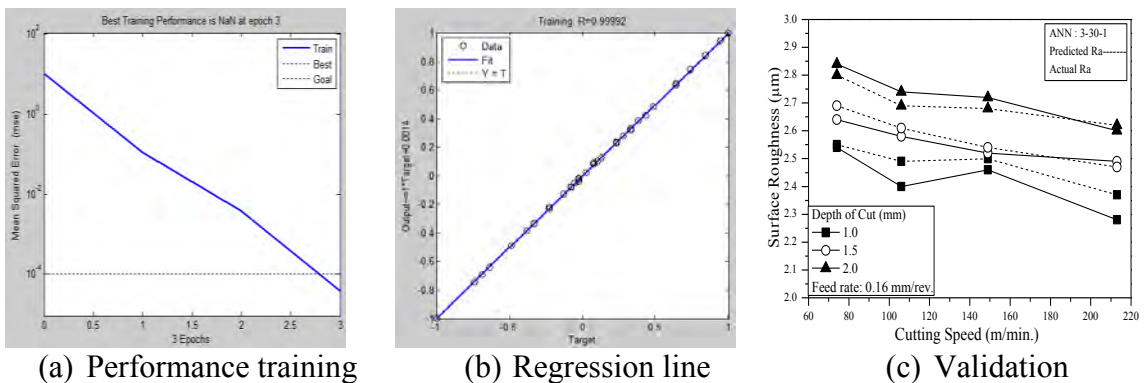


Fig. 4.6 Performance measure of 3-30-1 network

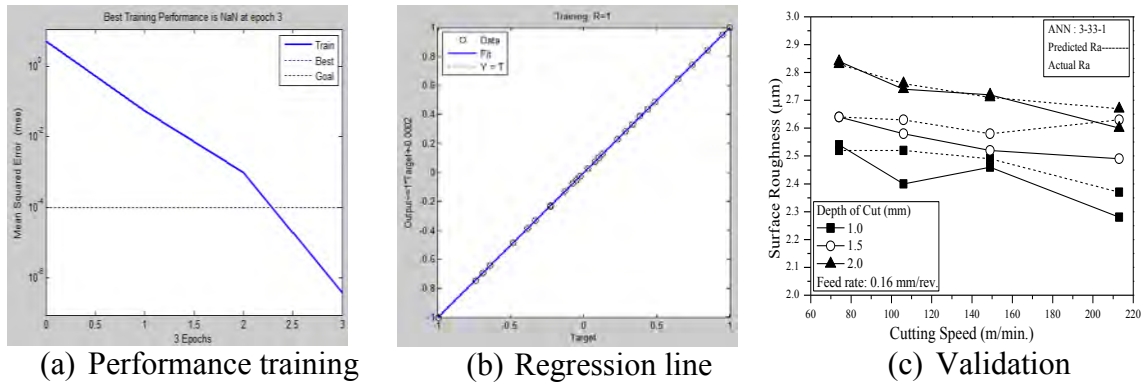


Fig. 4.7 Performance measure of 3-33-1 network

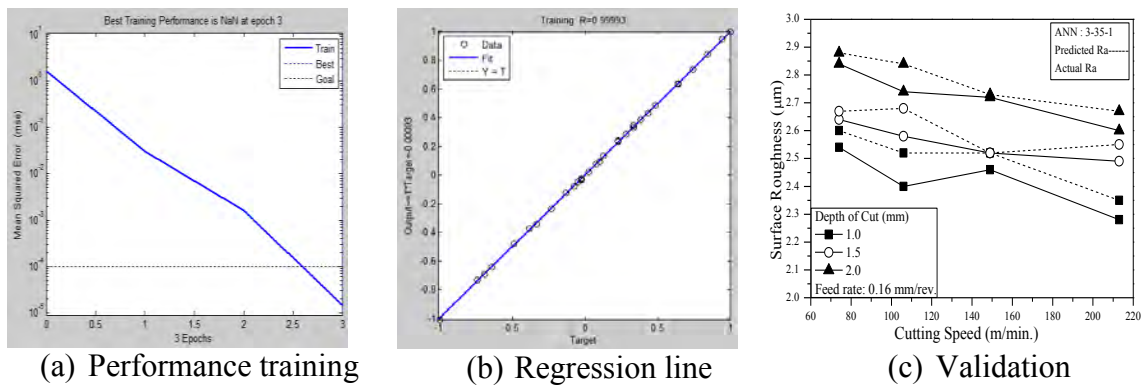


Fig. 4.8 Performance measure of 3-35-1 network

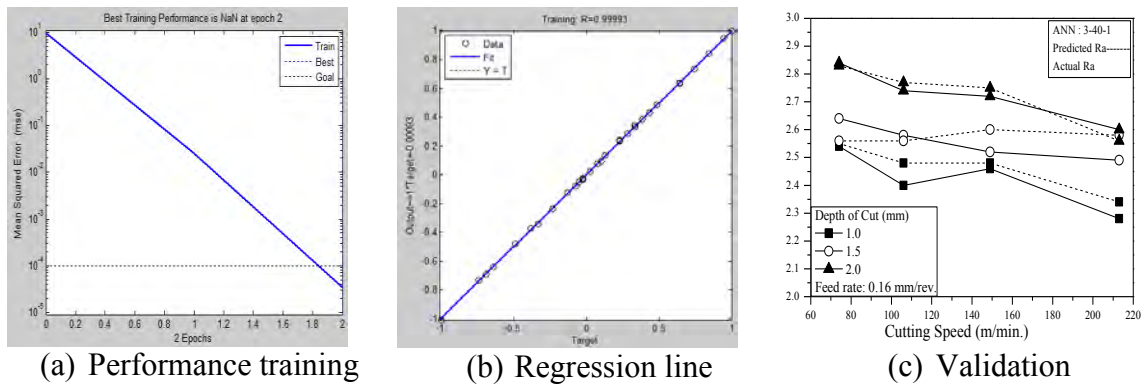


Fig. 4.9 Performance measure of 3-40-1 network

After post processing the predicted values using the MATLAB command `_postmnmx`, regression analysis was adopted to find the coefficient of determination value (R^2) for both training and testing phases to assess the network performance. The performance capability of each network was examined based on the coefficient of determination value (R^2) between the network predictions and the experimental values using the training and test data set. Finally, the optimal network was selected after testing with varying number of neurons in the hidden layers. For the obtained optimal network

architecture, hyperbolic tangent sigmoid ‘tansig’ transfer function was used in the hidden layer and linear transfer function ‘purelin’ was used in the output layer. Number of hidden neurons was 33. The performance of the network was evaluated by mean sum of squared error (MSE) between the measured and the predicted values for every output nodes in respect of training the network. The optimal network was chosen based on the minimum mean absolute percentage of error (MAPE). Table 4.2 presents the validation of the ANN model with respect to the experimental findings regarding the surface roughness of machined hybrid composite. Both the value of R^2 and MAPE for training and testing are also provided in the table.

Table 4.2 R^2 and MAPE values between the network predictions and the experimental values using training and test dataset

Training algorithm: Levenberg-Marquardt algorithm						
Transfer function : Tangent sigmoid ‘tansig’ transfer function and linear transfer function ‘purelin’ in the hidden and the output layer respectively						
	Training performance			Testing performance		
Hidden layer	1	1	1	1	1	1
Neurons in the layer	20	25	30	20	25	30
R_a (Surface roughness)						
R^2	0.99998	0.99999	0.99984	0.9435	0.9773	0.8590
MAPE	0.1622	0.0197	0.0813	2.8361	1.4177	3.3731
Hidden layer	1	1	1	1	1	1
Neurons in the layer	33	35	40	33	35	40
R_a (Surface roughness)						
R^2	1	0.99986	0.99986	0.9975	0.9815	0.7825
MAPE	0.0029	0.0013	0.0047	0.9527	1.5422	10.5056

Table 4.3 presents the optimal network architecture whereas Table 4.4 presents the summary of the optimal network architecture.

Table 4.3 Optimal Network from ANN

Network	: 3-33-1
Transfer Functions	: Tansig (hidden layer) : Purelin (Output layer)
MAPE _{train}	: 0.0029
MAPE _{test}	: 0.9527

Table 4.4 Summary of the ANN model for 3-33-1 ANN architecture for surface roughness prediction of Kevlar and glass fiber reinforced polyester

Type of neural network	: Multi layer feed-forward
	: Cutting speed, V_c (m/min.)
Input neurons	: Feed rate, S_o (mm/rev.)
	: Depth of cut, t (mm)
Output neuron	: Average surface roughness (R_a)
Number of Hidden layer	: 1
Hidden neurons	: 33
Learning algorithm	: Levenberg- Marquardt Optimization
Learning scheme	: Supervised learning
Learning rule	: Gradient descent rule
Transfer function	: Tangent sigmoid (Hidden layer)
	: Linear transfer function (Output layer)
Sample pattern vector	: 36 (for training) and 12 (for testing)
Learning rate	: 0.5
Momentum constant	: 0.5
All input data normalized between -1 and +1	
Number of epochs taken	: 3

Chapter-5

Discussion on Results

5.1 Cutting Force

Cutting force is one of the key concerns of any machining process. Cutting force along with other machining responses such as surface roughness, tool wear, temperature generation etc. are attributable to the product quality, functionality and production cost associated with machining. Cutting force increases with the increase of the material strength, shear strength to be specific. Increase of cutting force during machining is always detrimental for the process performance as it increases the temperature generation which leads to decreased tool life and increased surface roughness. Numerous researches have been carried out to decrease the magnitude of the cutting force during machining of metals and comparatively lesser works have also been performed on composite materials as well.

According to the graphical representations of the variation of main cutting force with feed rate, it is evident that for almost every cutting condition; reasonable values of cutting force are found. Fig. 3.2 affirms that the trend mainly shows increased cutting force with increased feed rate regardless of the machining environment. Again, for a particular feed, cutting force is mainly decreased with increased cutting speed. One anomaly is found while the part was machined under feed rate of 0.14 mm/rev., speed of 213 m/min and depth of cut of 1 mm. It gave a lesser value of cutting force than a feed rate of 0.12 mm/rev. as opposed to any other result of cutting force. According to Fig 3.3 while the material was turned under a depth of cut of 1.5 mm one deviation of the trend is found again that under speed of 213 m/min and depth of cut of 1.5 mm. It shows a lesser value of cutting force at a feed rate of 0.14mm/rev. than a feed rate of 0.12 mm/rev. This deviation has not been found in the case of any other cutting condition. The trend of cutting force was increasing with increased feed rate regardless of the cutting speed. Combining both of the environments along with all the cutting conditions, compressed air cooling provided

the best result under 213 m/min. cutting speed. According to Fig 3.4, when the material was turned under a depth of cut of 2 mm, everything went as it should have. Main cutting force mainly increased with increased feed rate and decreased with increased cutting speed. The least value of cutting force was found under a cutting speed of 213 m/min. and feed rate of 0.10 mm/rev. One notable thing was that for increased depth of cut the value of the cutting force increased drastically. The reason is with increased depth of cut, the cutting tool penetrates more and removes more amount of material resulting increased cutting force. With varying feed and keeping the cutting speed constant, the optimal result was obtained when the material was machined under cutting speed of 213 m/min. and feed rate of 0.10 mm/rev. and depth of cut of 1 mm. The reason of increased cutting force with increased feed is that more amount of material is cut per revolution of the workpiece and this requires higher amount of energy which ultimately leads to generate higher cutting force.

Fig. 3.5 to Fig. 3.7 mainly displays the variation in main cutting force with varying cutting speed while feed rate is kept constant. It is evident as Fig. 3.5 presents, for almost every cutting condition reasonable values of cutting force are found regardless of the machining environment. The trend of cutting force is mainly decreasing with increased cutting speed. Again, when the feed rate is in concern, cutting force mainly increased with increased feed regardless the values of cutting speed. Compressed air cooling provided the best result under 213 m/min. cutting speed and 0.10 mm/rev. feed rate and a depth of cut of 1 mm. A notable thing was that for increased depth of cut the value of the cutting force increased drastically but the trend of cutting force remains same with the variation of cutting speed. Again another important thing to remember is that, in any machining process with the increase in cutting speed, shearing of the material becomes a very easy phenomenon and during the experiment the higher the cutting speed was the easier the shear became which generated lesser cutting force.

When the results of two machining environments are compared to each other, it is found that compressed air cooling condition has produced much better result than dry condition in terms of lower cutting force as presented in Fig. 3.2 to Fig. 3.7. The degree of improvement in cutting force under compressed cooling was not consistent in all the cutting conditions but lower cutting forces were found nonetheless. Table 5.1 presents the

reduction in main cutting force while the material was machined under compressed air cooling condition in comparison to dry cutting condition. It is found that for each and every cutting speed, feed rate and depth of cut combination the reduction in cutting force is more than 5 percent and in some cases the reduction is more than 10 percent. In one case, there was no improvement in cutting force which was 36 N for both the machining environment and the cutting speed was 149 m/min., feed rate 0.12 mm/rev. and 1.5 mm depth of cut. The reason behind improvement of cutting force under compressed air cooling is mainly due to the continuous cooling of chip tool interface. In the case of dry cutting, the tool became hot and natural cooling process of convection took place in the cooling of cutting tool but in the case of compressed air cooling the tool was forced to be cooled by compressed air. Again, the more the compressed cooled air jet reached into the cutting zone correctly the cooler the tool became and it might have reduced the main cutting force in a considerable amount. The process of forced cooling helped the machining process to get a lower value of cutting force as well as lesser temperature generation.

Very few anomalies have been found during machining which do not conform to established knowledge to the machining of steels and FRP composites. Since, composite materials possess at least two different materials suggesting two materials that have completely different sets of mechanical and thermal properties, complex phenomenon can often occur during their machining. Different materials can also have different amount of thermal expansion during machining which can lead to unexpected results sometimes. Result also depends on how well the work material has been manufactured such as blow hole, pin hole etc. can deteriorate the machining quality. The developed hybrid composite material contained three different kinds of materials which were Kevlar, glass and polyester resin. These three materials have three different sets of mechanical and thermal properties and during the machining process of any kind thermal stress and flexural stress takes place in the work material. The combination of these stresses and the different mechanical and the thermal properties of the constituents of work material really makes the machining a difficult task and led to few unexpected results. Table 5.1 presents the percentage reduction in cutting force due to the usage of compressed air cooling in comparison to dry cutting.

Table 5.1 Percentage Reduction in main cutting force due to compressed air cooling

t (mm)	V _c (m/min.)	S _o (mm/rev.)	Environment		% reduction in P _z
			Dry	Compressed Air	
			P _z (N)	P _z (N)	
1.0	74	0.10	28	26	7.14
		0.12	31	30	3.23
		0.14	33	31	6.06
		0.16	34	32	5.88
	106	0.10	27	25	7.41
		0.12	30	29	3.33
		0.14	32	30	6.25
		0.16	33	31	6.06
	149	0.10	26	24	7.69
		0.12	29	28	3.45
		0.14	31	29	6.45
		0.16	32	30	6.25
	213	0.10	24	23	4.17
		0.12	26	25	3.85
		0.14	28	25	10.71
		0.16	29	26	10.34
1.5	74	0.10	37	34	8.11
		0.12	39	37	5.13
		0.14	41	40	2.44
		0.16	42	41	2.38
	106	0.10	36	34	5.56
		0.12	37	36	2.70
		0.14	40	39	2.50
		0.16	41	40	2.44
	149	0.10	35	33	5.71
		0.12	36	36	0.00
		0.14	39	37	5.13
		0.16	40	39	2.50
	213	0.10	34	31	8.82
		0.12	35	33	5.71
		0.14	36	33	8.33
		0.16	37	34	8.11
2.0	74	0.10	48	47	2.08
		0.12	50	48	4.00
		0.14	50	49	2.00
		0.16	52	51	1.92
	106	0.10	46	43	6.52
		0.12	49	46	6.12
		0.14	50	48	4.00
		0.16	51	49	3.92
	149	0.10	44	42	4.55
		0.12	46	45	2.17
		0.14	48	46	4.17
		0.16	49	47	4.08
	213	0.10	42	41	2.38
		0.12	44	42	4.55
		0.14	45	43	4.44
		0.16	46	44	4.35

5.2 Surface Roughness

The surface integrity of a work material is one of the main determinants of its functional ability throughout its service life. A significant proportion of component failure starts at the surface due to either an isolated manufacturing discontinuity or gradual deterioration of the surface quality. Variations in the surface texture can influence a variety of performance characteristics. The surface finish can affect the ability of the part to resist wear and fatigue; to assist effective lubrication; to affect friction and/or abrasion with mating parts; and to resist corrosion, increase in surface finish improves reflective properties. As these characteristics become critical under certain operating conditions, the surface finish can dictate the performance, integrity and service life of the component. In the case of steels, cutting fluid improves the surface integrity of work material. As application of cutting fluid reduces the temperature generation, leading to less wear of the tool, the surface finish of the work material improves. However, conventional cutting fluid cannot be used for machining a composite material as it deteriorates the mechanical property of the material itself. So, in machining FRPs, only cryogenic cooling or compressed air cooling condition could be provided. In this thesis during the experimental investigation, the later one was used and it has improved the surface roughness in a number of ways. For the investigative study of machining of hybrid composite, surface roughness was considered as the main parameter to define quality of the machined work material under both dry and compressed air cooling condition.

Surface roughness is defined as irregular deviations on a scale smaller than the scale of waviness. In other words, surface roughness is described as irregularities wrought by different machining processes [Mahdavinejad et al. 2012]. Again, surface roughness has also been defined as the superimposition of deviations from a nominal surface from the third to the sixth order where the orders of deviations are defined by the international standards [Bernados and Vosniakos 2003]. Deviations of first and second order are related to form; consisting of flatness, circularity, waviness etc. These deviations are due to machine tool errors, deformation of the workpiece, erroneous setups, vibration and workpiece inhomogenities etc. Deviations of third and fourth order consist of periodic grooves, cracks and dilapidations are they occur because of shape and conditions of cutting edges, chip formation and process kinematics. Deviations of fifth and sixth orders are

linked to workpiece material structure and are related to physico- chemical mechanisms acting on a grain and lattice scale such as slip, diffusion, oxidation and residual stresses.

According to the graphical representations of variation of surface roughness in different cutting conditions, it is evident that for almost every cutting condition, reasonable surface roughness is found. From Fig. 3.8, it is evident that the trend of surface roughness is mainly increasing with increased feed rate indifferent of the cutting speed. One deviation is found from the graphical representation where the workpiece was machined under compressed air cooling condition with a speed of 74 m/min., depth of cut of 1 mm. It is noticed that 0.14 mm/rev. feed produced lesser surface roughness than 0.12 mm/rev. which was conflicting to any other cutting condition regardless of the machining environment. According to Fig. 3.9, there is a clear increasing trend of surface roughness with increasing feed rate regardless of the cutting speed at which the material was machined. Fig. 3.10 also manifests an increasing trend of surface roughness with increasing feed rate. For a particular cutting speed, the surface roughness was increasing as long as the feed went onto increase. The higher the feed, the more the tool covers an axial distance per revolution of the workpiece and wavy surfaces tend to produce.

When the cutting speed is in concern, surface roughness is mainly decreased with increased cutting speed regardless the values of feed as shown from Fig. 3.11 to Fig. 3.13. Each one of the graph of surface roughness vs. cutting speed showed without any major deviation from the trend that with increasing cutting speed, surface roughness is decreased regardless of the feed rate. With increased cutting speed the deformation of the work material becomes very easy and in general a lower surface roughness is produced. In this investigation, lower surface roughness is found in general with increased speed and easy deformation of the work material might have worked as a reason. Few anomalies to the established knowledge of machining metals have been found but since composite is inhomogeneous its fiber distribution may not be well distributed within the matrix and where there was inequality in fiber distribution there some anomalies might have occurred during the machining operation. Again another important thing to notice was the increase of surface roughness with the increase in depth of cut. It is obtained from the figures, maximum depth of cut produced maximum surface roughness, the reason might be that

due to the increase in cutting force and higher tool wear also took place with increased depth of cut and deteriorated the surface quality.

Again when the results of two machining environments were compared to each other, it is found compressed air cooling condition has produced better result than dry condition in terms of lower surface roughness as presented from Fig. 3.8 to Fig. 3.13. The degree of improvement in surface roughness under compressed cooling is not consistent in all the cutting conditions but lower values of surface roughness were found nonetheless. Table 5.2 presents the reduction in surface roughness while the material was machined under compressed air cooling condition in comparison to dry cutting condition. It is noticeable that for each and every cutting condition, the reduction in surface roughness is more than 2 percent and in some cases the reduction is more than 5 percent. The improvement of surface roughness under compressed air cooling was mainly due to the continuous cooling of chip tool interface in the cutting zone. In the case of dry cutting, the temperature grew continuously, natural cooling process of convection took place in the cooling of cutting tool but in the case of compressed air cooling the tool was forced to be cooled by compressed air. The forced cooling of chip tool interface gave a lower value of surface roughness and produced a better surface texture.

Because of composite materials anisotropy and non homogeneous characteristics some of the deviations were found. Anisotropic properties mainly occurred due to the blending of different materials to form a new material. The work material was developed by casting three different kinds of materials which were Kevlar, glass and polyester resin. These three materials have three different sets of mechanical and thermal properties and during the machining process of any kind, thermal stress and flexural stress take place in the work material. The combination of these stresses and the differential thermal expansion of the composite constituents really make the machining a difficult task. The complicated interaction between the three different materials was perhaps the main reason for showing no consistency in improvement of surface roughness. Table 5.2 presents the percentage reduction in surface roughness due to the usage of compressed air cooling in comparison to cutting in dry environment.

Table 5.2 Percentage Reduction in surface roughness due to compressed air cooling

t (mm)	V _c (m/min.)	S _o (mm/rev.)	Environment		% Reduction in R _a
			Dry	Compressed Air	
			R _a (μm)	R _a (μm)	
1.0	74	0.10	2.38	2.28	4.20
		0.12	2.46	2.42	1.63
		0.14	2.54	2.44	3.94
		0.16	2.62	2.54	3.05
	106	0.10	2.32	2.24	3.45
		0.12	2.36	2.34	0.85
		0.14	2.48	2.40	3.23
		0.16	2.52	2.48	1.59
	149	0.10	2.24	2.16	3.57
		0.12	2.32	2.30	0.86
		0.14	2.42	2.38	1.65
		0.16	2.44	2.46	0.82
	213	0.10	2.18	2.04	6.42
		0.12	2.26	2.14	5.31
		0.14	2.30	2.18	5.22
		0.16	2.36	2.28	3.39
1.5	74	0.10	2.54	2.48	2.36
		0.12	2.60	2.54	2.31
		0.14	2.62	2.58	1.53
		0.16	2.68	2.64	1.49
	106	0.10	2.50	2.47	1.20
		0.12	2.56	2.52	1.56
		0.14	2.60	2.56	1.54
		0.16	2.64	2.58	2.27
	149	0.10	2.42	2.40	0.83
		0.12	2.48	2.42	2.42
		0.14	2.52	2.46	2.38
		0.16	2.56	2.52	1.56
	213	0.10	2.38	2.34	1.68
		0.12	2.43	2.40	1.23
		0.14	2.46	2.41	2.03
		0.16	2.52	2.49	1.19
2.0	74	0.10	2.82	2.76	2.13
		0.12	2.86	2.80	2.10
		0.14	2.88	2.82	2.08
		0.16	2.92	2.84	2.74
	106	0.10	2.72	2.62	3.68
		0.12	2.76	2.68	2.90
		0.14	2.78	2.72	2.16
		0.16	2.82	2.74	2.84
	149	0.10	2.62	2.56	2.29
		0.12	2.68	2.60	2.99
		0.14	2.72	2.68	1.47
		0.16	2.78	2.72	2.16
	213	0.10	2.50	2.42	3.20
		0.12	2.58	2.52	2.33
		0.14	2.61	2.56	1.92
		0.16	2.66	2.60	2.26

5.3 Prediction of Surface Roughness Using ANN

Artificial neural networks (ANNs) are among the most powerful and largely used predictive modeling techniques based on statistical approach. This machine learning technique is currently being used in many fields of engineering for modeling complex relationships which are difficult to describe with physical models. It is also used in the areas where there are no authentic governing equations to describe a phenomenon.

The importance of predicting surface finish in any machining process help the engineers for proper planning, control of machining parameters and optimization of the cutting conditions to minimize production cost, time and manufacturing products of desired quality. The mentioned advantages eventually lead to higher productivity which is the main goal of any production or service based organization.

In this thesis, ANN model to predict surface roughness has been constructed for Kevlar and glass reinforced polyester turned under compressed air cooling condition. During the ANN modeling of surface roughness of the machined part, the input layer was chosen to contain three neurons specifically cutting speed, feed rate and depth of cut while the output neuron was surface roughness of the turned part. Between the input and the output layer, one hidden layer was chosen in the process. The hidden layer could contain different number of neurons and selecting the number of hidden neurons in the hidden layer was the main task to find the optimal neural network structure. Six different network structures were designed in order to choose the optimal network structure. The number of hidden neurons was chosen based on trial and error approach. The network structures were 3-20-1, 3-25-1, 3-30-1, 3-33-1, 3-35-1 and 3-40-1; where 3 stands for number of input neurons, 20, 25, 30, 33, 35, 40 stand for the number of neurons in the hidden layer and finally 1 stands for the number of output neuron. Each of the developed network structure was trained under the Levenberg Marquardt equation and for each one the network structure, the learning paradigm was supervised learning i.e. the target output was also provided during designing the network structures. Before training the network the values of the network input was normalized. Transfer functions used in the hidden layer and the output layer were `_tansig` transfer function and `_purelin` transfer function respectively. As mentioned earlier, the networks were trained with 36 combinations of surface roughness whereas tested against 12 combinations.

The network structures were trained and tested and their validation was also done as shown from Fig. 4.3 to Fig. 4.8. This validation was performed in order to justify the accuracy of the developed ANN model. Taking the experimental value of surface roughness and the values predicted by ANN, graphs were plotted as shown in the figures. They presented a comparison between the experimental and ANN predicted values of surface roughness. From Fig. 4.3, it is clearly evident that ANN almost predicted the experimental values accurately for each cutting condition. According to Fig. 4.4 few anomalies are there to predict surface roughness since it was not in a very good agreement with experimental results as suggested by Fig. 4.3. One deviation is found in the predicted values while cutting under a speed of 106 m/min. and depth of cut of 1 mm. From Fig. 4.5, the network containing 30 neurons in the hidden layer was able to predict the surface roughness almost accurately for all the cutting conditions. From Fig. 4.6, where the hidden layer contained 33 neurons is almost accurate in predicting surface roughness but two deviations were found nonetheless. Firstly, while the workpiece was machined under a speed of 106 m/min., depth of cut of 1 mm and secondly while the workpiece was machined under a speed of 213 m/min. depth of cut of 1.5 mm. According to Fig. 4.7 and Fig. 4.8, the prediction is not good enough to follow the trend of surface roughness with experimental values but nonetheless the test error within reasonable limits for the network structure containing 35 neurons. Only the network structure containing 40 neurons has produced a test error of more than 10% and the rest of them were well accurate to predict the desired surface roughness.

After taking the predicted values of the six different structures, the optimal network was chosen. The desired optimal network was chosen based on the minimum value of mean absolute percentage of error (MAPE). It was found that 3-33-1 structure provided the least value of MAPE and both of its train error and test error was lesser than the other designed networks. The train error of the optimal network was 0.0029 and its test error was 0.9527.

Because of composite materials non homogeneous characteristics these anomalies were found. The developed work material contained three different kinds of materials which were Kevlar, glass and polyester resin. These three materials have three different sets of mechanical and thermal properties and during the machining process of any kind

thermal stress and flexural stress takes place in the work material. The combination of these stresses and the different mechanical and the thermal properties of the constituents of work material really makes the machining a difficult task. So, unlike metals the predictions of the surface roughness and other machining responses are a complicated task to accomplish for any machine learning process. Again, Kevlar fibers in FRP composites always tend to pull out during machining and damage the surface integrity severely but by reinforcing the same matrix with both Kevlar and glass fiber, the above mentioned problem was solved.

An important parameter vibration was not considered in order to keep the network simple and convenient for constructing but it might have affected the machining process and because of these, ANN model may have failed to predict the surface roughness accurately in some cases.

Nevertheless, the developed ANN model was good enough to keep prediction error well below 10 percent for different cutting conditions except 3-40-1. In the case of 3-40-1 network the test was found to be 10.5056 which suggests, this network should not be used for predicting surface roughness of the turned part as the error above 10%. The optimal network found to be 3-33-1 based on mean absolute percentage of error. Table 5.3 provides the cutting condition, experimental surface roughness, predicted surface roughness by ANN and the train and the test error of the developed network structure.

Table 5.3 Actual value of R_a versus prediction by ANN

Cutting Condition			Experimental R_a	Predicted R_a	ANN model	MAPE _{train}	MAPE _{test}
V_c	S_o	t					
74	0.16	1.0	2.54	2.52	3-20-1	0.1622	2.8361
106	0.16	1.0	2.40	2.45			
149	0.16	1.0	2.46	2.48			
213	0.16	1.0	2.28	2.37			
74	0.16	1.5	2.64	2.65			
106	0.16	1.5	2.58	2.62			
149	0.16	1.5	2.52	2.58			
213	0.16	1.5	2.49	2.53			
74	0.16	2.0	2.84	2.80			
106	0.16	2.0	2.74	2.75			
149	0.16	2.0	2.72	2.69			
213	0.16	2.0	2.60	2.65			
74	0.16	1.0	2.54	2.55	3-25-1	0.0197	1.4177
106	0.16	1.0	2.40	2.53			
149	0.16	1.0	2.46	2.48			
213	0.16	1.0	2.28	2.37			
74	0.16	1.5	2.64	2.65			
106	0.16	1.5	2.58	2.63			
149	0.16	1.5	2.52	2.57			
213	0.16	1.5	2.49	2.52			
74	0.16	2.0	2.84	2.82			
106	0.16	2.0	2.74	2.74			
149	0.16	2.0	2.72	2.67			
213	0.16	2.0	2.60	2.64			
74	0.16	1.0	2.54	2.55	3-30-1	0.0813	3.3731
106	0.16	1.0	2.40	2.49			
149	0.16	1.0	2.46	2.50			
213	0.16	1.0	2.28	2.37			
74	0.16	1.5	2.64	2.69			
106	0.16	1.5	2.58	2.61			
149	0.16	1.5	2.52	2.54			
213	0.16	1.5	2.49	2.47			
74	0.16	2.0	2.84	2.80			
106	0.16	2.0	2.74	2.69			
149	0.16	2.0	2.72	2.68			
213	0.16	2.0	2.60	2.62			
74	0.16	1.0	2.54	2.52	3-33-1	0.0029	0.9527
106	0.16	1.0	2.40	2.52			
149	0.16	1.0	2.46	2.49			
213	0.16	1.0	2.28	2.37			
74	0.16	1.5	2.64	2.64			
106	0.16	1.5	2.58	2.63			
149	0.16	1.5	2.52	2.58			
213	0.16	1.5	2.49	2.63			
74	0.16	2.0	2.84	2.83			
106	0.16	2.0	2.74	2.76			
149	0.16	2.0	2.72	2.71			
213	0.16	2.0	2.60	2.67			

Cutting Condition			Experimental	Predicted	ANN model	MAPEtrain	MAPEtest
V _c	S ₀	t	R _a	R _a			
74	0.16	1.0	2.54	2.60	3-35-1	0.0013	1.5422
106	0.16	1.0	2.40	2.52			
149	0.16	1.0	2.46	2.52			
213	0.16	1.0	2.28	2.35			
74	0.16	1.5	2.64	2.67			
106	0.16	1.5	2.58	2.68			
149	0.16	1.5	2.52	2.52			
213	0.16	1.5	2.49	2.55			
74	0.16	2.0	2.84	2.88			
106	0.16	2.0	2.74	2.84			
149	0.16	2.0	2.72	2.73			
213	0.16	2.0	2.60	2.67			
74	0.16	1.0	2.54	2.55			
106	0.16	1.0	2.40	2.48			
149	0.16	1.0	2.46	2.48			
213	0.16	1.0	2.28	2.34			
74	0.16	1.5	2.64	2.56			
106	0.16	1.5	2.58	2.56			
149	0.16	1.5	2.52	2.60			
213	0.16	1.5	2.49	2.58			
74	0.16	2.0	2.84	2.83			
106	0.16	2.0	2.74	2.77			
149	0.16	2.0	2.72	2.75			
213	0.16	2.0	2.60	2.56			

Conclusions and Recommendations

From the machining investigation and the ANN the modeling of surface roughness of hybrid composite following conclusions can be drawn.

Conclusions

- i. In depth investigation of the machinability of Kevlar and glass reinforced polyester has been performed under both dry and compressed cooling air condition from the perspectives of surface roughness and cutting force.
- ii. Surface roughness has been found to improve while the work was turned under compressed air cooling in comparison that of dry machining.
- iii. Different cutting condition provided different degrees of improvements. In terms of surface roughness, the best result was obtained under compressed air cooled environment when the cutting speed was 213 m/min., feed 0.10 mm/rev. and depth of cut was 1 mm. The value of the surface roughness was 2.04 μm .
- iv. The maximum surface roughness was found under dry condition when the cutting speed was 74 m/min., feed 0.16 mm/rev. and depth of cut was 2 mm. The value of the maximum surface roughness was found to be 2.92 μm .
- v. Cutting force was also substantially reduced while machined under compressed air cooling environment as compared to that of dry machining.
- vi. Again, different cutting condition showed different degree of improvements. When cutting force was in concern, the best result was found under compressed air cooled environment when the cutting speed was 213 m/min., feed 0.10 mm/rev. and depth of cut was 1 mm. The value of the minimum cutting force was found to be 23 N.

- vii. The maximum main cutting force was found under dry condition when the cutting speed was 74 m/min., feed 0.16 mm/rev. and depth of cut was 2 mm. The value of the cutting force obtained was 52 N.
- viii. Surface roughness of the machined part has been modeled using artificial neural network. Six successful networks were designed containing different number of hidden neurons. Optimum network had one hidden layer containing 33 neurons. Hyperbolic tangent sigmoid `_tansig'` transfer function and linear output transfer function `_purelin'` have been selected for hidden layer and output layer respectively. The optimal network showed a mean absolute train error of 0.0029 where the mean absolute test error was 0.9527.

Recommendations

- i. Investigations in turning hybrid composite can be carried out with different compositions of the fibrous materials. Different matrix materials can also be introduced to observe the impact of different cutting conditions on their machinability.
- ii. In this thesis, machinability study of hybrid composite has been performed under only dry and compressed cooling condition but it can also be carried out under cryogenic cooling environment.
- iii. During the machining operation; cutting speed, feed and depth of cut were changed but nozzle inclination angle, machining time as well as different kinds of cutting inserts such as CBN, PCDs can also be used to assess hybrid composites' machinability.
- iv. In the present work, an artificial neural network model has been constructed to predict surface roughness by using 48 combinations of surface roughness. However, network inputs parameters can be increased along with network output. The more the training and testing data will be available, the more the accurate network will be.
- v. Again, modeling of surface roughness can also be done using other recognized techniques such as ANFIS, RSM, MRA etc. Also, a competitive comparison can also be presented among the modeling techniques.

References

- Abrão, A.M., Faria, P.E., Rubio, J.C.C., Reis, P. and Davim, J.P., Drilling of Fiber Reinforced Plastics: A Review, *Journal of Materials Processing Technology*, Vol. 186(1-3), pp.1–7, 2007
- Andrews, M.C., Lu, D. and Young, R.J., Compressive Properties of Aramid Fibers, *Polymer*, Vol. 38(10), pp.2379–2388, 1997
- Asiltürk, I., Predicting Surface Roughness of Hardened AISI 1040 Based on Cutting Parameters Using Neural Networks and Multiple Regression, *International Journal of Advanced Manufacturing Technology*, Vol. 63(1-4), pp.249-257, 2012
- Azmi, A.I., Multi-Objective Optimization of Machining Fibre Reinforced Composites, *Journal of Applied Sciences*, Vol. 12(23), pp.2360-2367, 2012
- Azmi, A.I., Lin, R.J.T. and Bhattacharyya D., Machinability Study of Glass Fibre-Reinforced Polymer Composites During End Milling, *International Journal of Advanced Manufacturing Technology*, Vol. 64(1-4), pp.247-261, 2013
- Bagci, E. and İşık, B., Investigation of Surface Roughness in Turning Unidirectional GFRP Composites by Using RS Methodology and ANN, *International Journal of Advanced Manufacturing Technology*, Vol. 31(1-2), pp.10-17, 2006
- Benardos, P.G. and Vosniakos, G.C., Predicting surface roughness in machining: a review, *International Journal of Machine Tools and Manufacture*, Vol. 43(8), pp.833–844, 2003
- Bhattacharya, D., Allen, M.N. and Mander, S.J., Cryogenic Machining of Kevlar Composites, *Materials and Manufacturing Processes*, Vol. 8(6), pp.631-651, 1993

- Bhattacharyya, D. and Horrigan, D.P.W., A Study of Hole Drilling In Kevlar Composites, Composites Science and Technology, Vol. 58(2), pp.267–283 ,1998
- Bhushan, K.R., Kumar, S. and Das, S., Effect of Machining Parameters on Surface Roughness and Tool Wear for 7075 Al Alloy SiC Composite, International Journal of Advanced Manufacturing Technology, Vol. 50(5-8), pp.459-469, 2010
- Brezocnik, M. and Kovacic, M., Integrated Genetic Programming and Genetic Algorithm Approach to Predict Surface Roughness, Materials and Manufacturing Processes, Vol. 18(3), pp.475-491, 2003
- Brinksmeier, E. and Janssen, R., Drilling of Multi-Layer Composite Materials consisting of Carbon Fiber Reinforced Plastics (CFRP), Titanium and Aluminum Alloys, CIRP Annals - Manufacturing Technology, Vol. 51(1), pp.87–90, 2002
- Bunsell, A.R., The Tensile and Fatigue Behavior of Kevlar-49 (PRD-49) Fiber, Journal of Material Science, Vol. 10(8), pp.1300-1308, 1975
- Chen, J.C. and Savage, M., A Fuzzy Net Based Multi Level in Process Surface Recognition System in Milling Operations, International Journal of Advanced Manufacturing and Technology, Vol. 17(9), pp.670-676, 2001
- Dandekar, C.R. and Shin, Y.C., Modeling of Machining of Composite Materials: A Review, International Journal of Machine Tools and Manufacture, Vol. 57, pp.102–121, 2012
- Davim, J.P. and Mata, F., Optimization of Surface Roughness on Turning Fiber-Reinforced Plastics (FRPs) With Diamond Cutting Tools, International Journal of Advanced Manufacturing Technology, Vol. 26(4), pp.319-323, 2004
- Davim, J.P. and Mata, F., A Comparative Evaluation of the Turning of Reinforced and Unreinforced Polyamide, International Journal of Advanced Manufacturing Technology, Vol. 33(9-10), pp.911-914, 2007

- Dhar, N., Islam, S., Kamruzzaman, M., Effect of Minimum Quantity Lubrication (MQL) on Tool Wear, and Dimensional Deviation in Turning Aisi-4340 Steel. *G. U. Journal of Science*, pp.23–32, 2007
- Dureja, J.S., Singh, R., Singh, T., Singh, P., Dogra, M. and Bhatti, M.S., Performance Evaluation of Coated Carbide Tool In Machining of Stainless Steel (AISI 202) Under Minimum Quantity Lubrication (MQL), *International Journal of Precision Engineering and Manufacturing-Green Technology*, Vol. 2(2), pp.123-129, 2015
- Escalona, P.M. and Maropoulos, P.G., Artificial Neural Networks for Surface Roughness Prediction when Face Milling Al 7075-T7351, *Journal of Materials Engineering and Performance*, March 2010, Vol. 19(2), pp.185-193, 2010
- Ganczakowski, H.L. and Beaumont, P.W.R., The Behavior of Kevlar Fiber-Epoxy Laminates Under Static and Fatigue Loadings. Part I—Experimental, *Composite Sciences and Technology*, Vol. 36(4), pp.299–319, 1989
- Gill, S.K., Gupta, M. and Satsangi, P.S., Prediction of Cutting Forces in Machining of Unidirectional Glass Fiber Reinforced Plastics Composite, *Frontiers of Mechanical Engineering*, Vol.8(2), pp.187-200, 2013
- Greenwood, J.H. and Rose, P.H., Compressive Behavior of Kevlar 49 Fibers and Composites, *Journal of Materials Science*, Vol. 9(11), pp.1809-1814, 1974
- Gustin, J., Joneson, A., Mahinfalah, M. and Stone, J., Low Velocity Impact of Combination Kevlar/Carbon Fiber Sandwich Composites, *Composite Structures*, Vol. 69(4), pp.396–406, 2005
- Hearle, J.W.S. and Wong, B.S., Flexural Fatigue and Surface Abrasion of Kevlar-29 and other High-Modulus Fibers, *Journal of Materials Science*, Vol. 12(12), pp.2447-2455, 1977
- Ho, S.N. and Suh, N.P., Effect of Fiber Orientation on Friction and Wear of Fiber Reinforced Polymeric Composites, *Wear*, Vol. 53(1), pp.129–141, 1979

- Ho, W.H., Tsai, J.T., Lin, B.T. and Chou, J.H., Adaptive Network Based Fuzzy Inference System for Prediction of Surface Roughness in End Milling Process Using Hybrid Taguchi Genetic Learning Algorithm, *Expert Systems with Applications*, Vol. 36(2), pp.3216–3222, 2009
- Isik, B., Experimental Investigations of Surface Roughness in Orthogonal Turning of Unidirectional Glass-Fiber Reinforced Plastic Composites, *International Journal of Advanced Manufacturing Technology*, Vol. 37(1-2), pp.42-48, 2007
- Karayel, D., –Prediction and Control of Surface Roughness in CNC Lathe Using Artificial Neural Network”, *Journal of Materials Processing Technology*, Vol. 209(7), pp. 3125–3137, 2009
- Kok, M., Modeling the Effect of Surface Roughness Factors in the Machining Of 2024Al/Al₂O₃ Particle Composites Based on Orthogonal Arrays, *International Journal of Advanced Manufacturing Technology*, Vol. 55(9-12), pp.911-320, 2011
- Komanduri, R., Zhang, B. and Vissa, C.M., Machining of Fiber Reinforced Composite, *Proc. Conference on Processing and Manufacturing of Composites*, ASME, pp. 1-36, 1991
- Kumanan, S., Jesuthanam, C.P. and Kumar R.A., Application of multiple regression and adaptive neuro fuzzy inference system for the prediction of surface roughness, *International Journal of Advanced Manufacturing Technology*, Vol. 35(7-8), pp.778-788, 2008
- Kumar, S., Meenu, Satsangi, P.S., Multiple-Response Optimization of Turning Machining By the Taguchi Method and the Utility Concept Using Uni-Directional Glass Fiber-Reinforced Plastic Composite and Carbide (K10) Cutting Tool, *Journal of Mechanical Science and Technology*, Vol. 27(9), pp.2829-2837, 2013
- Lela, B., Bajić, D. and Jozić, S., Regression Analysis, Support Vector Machines, and Bayesian Neural Network Approaches to Modeling Surface Roughness in Face Milling, *International Journal of Advanced Manufacturing Technology*, Vol. 42(11), pp.1082-1088, 2009

- Lin, S.C. and Chen, I.K., Drilling Carbon Fiber- Reinforced Composite Material at High Speed, *Wear*, Vol. 194(1-2), pp.156–162, 1996
- Lo, S.P., An Adaptive-Network Based Fuzzy Inference System for Prediction of Workpiece Surface Roughness in End Milling, *Journal of Materials Processing Technology*, pp.665–675, 2003
- Mahdavinejad, R.A., Khani N. and Fakhrabadi M.M.S., Optimization of Milling Parameters Using Artificial Neural Network and Artificial Immune System, *Journal of Mechanical Science and Technology*, Vol. 26(12), pp.4097-4104, 2012
- Marom, G., Drukker, E., Weinberg, A. and Banbaji J., Impact Behavior of Carbon/Kevlar Hybrid Composite, *Composites*, Vol. 9(1), pp.25–32, 1978
- Mittelman, A. and Roman, I., Tensile Properties of Real Unidirectional Kevlar/Epoxy Composites, *Composites*, Vol. 21(1), pp.63–69, 1990
- Natarajan, C., Muthu, S. and Karuppuswamy, P., Prediction and Analysis of Surface Roughness Characteristics of a Non-Ferrous Material Using ANN in CNC Turning, *International Journal of Advanced Manufacturing Technology*, Vol. 57(9-12), pp.1043-1051, 2011
- Oliveira, D.J., Guermandi, L.G., Bianchi, E.C., Diniz, A.E., Aguiar, P.R. and Canarim R.C., Improving Minimum Quantity Lubrication In CBN Grinding Using Compressed Air Wheel Cleaning, *Journal of Materials Processing Technology*, Vol. 212(12), pp. 2559–2568, 2012
- Özel, T. and Karpat, Y., Predictive Modeling of Surface Roughness and Tool Wear in Hard Turning Using Regression and Neural Networks, *International Journal of Machine Tools and Manufacture*, Vol. 45(4–5), pp. 467–479, 2005
- Pal, S.K. and Chakraborty, D., –Surface Roughness Prediction in Turning Using Artificial Neural Network”, *Neural Computing & Applications*, Vol. 14(4), pp.319-324, 2005
- Palanikumar, K., Application of Taguchi and Response Surface Methodologies for Surface Roughness in Machining Glass Fiber Reinforced Plastics by PCD Tooling,

International Journal of Advanced Manufacturing Technology, Vol. 36(1-2), pp.19-27, 2006

Persson, E., Ingvar, E. and Zackrisson, L., Effects of Hole Machining Defects on Strength and Fatigue Life of Composite Laminates, Composites Part A: Applied Science and Manufacturing, Vol. 28(2), pp.141–151, 1997

Qiu, Y. and Schwartz, P., Micromechanical Behavior of Kevlar-149/S-Glass Hybrid Seven-Fiber Microcomposites: I. Tensile Strength of The Hybrid Composite, Composites Science and Technology, Vol. 47(3), pp.303–315, 1993

Rahman, M., Ramakrishna, S., Prakash, J.R.S. and Tan, D.C.G., Machinability Study of Carbon Fiber Reinforced Composite, Journal of Materials Processing Technology, Vol. 89–90, pp.292–297, 1999

Raju, K.V.M.K., Janardhana, G.R., Kumar, P.N. and Rao, V.D.P., Optimization of Cutting Conditions for Surface Roughness in CNC End Milling, International Journal of Precision Engineering and Manufacturing, Vol. 12(3), pp.383-391, 2011

Rishbood, K.A., Dixit, U.S. and Sahasrabudhe, A.D., Prediction of Surface Roughness and Dimensional Deviation by Measuring Cutting Forces and Vibrations in Turning Process, Journal of Materials Processing Technology, Vol. 132(1–3), pp.203–214, 2003

Sahin, Y. and Motorcu, A.R., Surface Roughness Model for Machining Mild Steel With Coated Carbide Tools, Materials & Design, Vol. 26(4), pp.321–326, 2005

Santhanakrishnan, G., Krishnamurthy, R. and Malhotra, S.K., Machinability Characteristics of Fibre Reinforced Plastics Composites, Journal of Mechanical Working Technology, Vol. 17, pp.195–204, 1988

Santhanakrishnan, G., Krishnamurthy, R. and Malhotra S.K., High Speed Steel Tool Wear Studies in Machining of Glass-Fiber-Reinforced Plastics, Wear, Vol. 132(2), pp.327–336, 1989

- Shababi, H.H. and Ratnam, M.M., Prediction of Surface Roughness and Dimensional Deviation of Workpiece in Turning: A Machine Vision Approach, *International Journal of Advanced Manufacturing Technology*, Vol. 48(1-4), pp.213-226, 2010
- Shahrajabian, H. and Farahnakian, M., Modeling and Multi-Constrained Optimization in Drilling Process of Carbon Fiber Reinforced Epoxy Composite, *International Journal of Precision Engineering and Manufacturing*, Vol. 14(10), pp.1829-1837, 2013
- Sharma, V.S., Dhiman, S., Sehgal, R. and Sharma S.K., Estimation of Cutting Forces and Surface Roughness for Hard Turning Using Neural Networks, *Journal of Intelligent Manufacturing*, Vol. 19(4), pp.473-483, 2008
- Singh, I. and Bhatnagar, N., Drilling of Uni-Directional Glass Fiber Reinforced Plastic (UD-GFRP) Composite Laminates, *International Journal of Advanced Manufacturing Technology*, Vol. 27(9-10), pp.870-876, 2006
- Sonbaty E., Khashaba U.A. and Machaly T., Factors Affecting the Machinability of GFR/Epoxy Composites, *Composite Structures*, Vol. 63(3-4), pp.329–338, 2004
- Sreenivasulu R., Optimization of Surface Roughness and Delamination Damage of GFRP Composite Material in End Milling Using Taguchi Design Method and Artificial Neural Network, *Procedia Engineering*, International Conference on Design and Manufacturing, Vol. 64, pp.785–794, 2013
- Subramanian M., Sakthivel M., Sudhakaran R., Modeling and Analysis of Surface Roughness of AL7075-T6 in End Milling Process Using Response Surface Methodology, *Arabian Journal for Science and Engineering*, Vol. 39(10), pp.7299-7313, 2014
- Tai, B.L., Stephenson, D.A., Furness, R.J. and Shih A.J., Minimum Quantity Lubrication (MQL) in Automotive Powertrain Machining, *Procedia CIRP*, Vol. 14, pp.523–528, 2014
- Tandon, S., Jain, V.K., Kumar, P. and Rajurkar, K.P., Investigations Into Machining of Composites, *Precision Engineering*, Vol. 12(4), pp.227–238, 1990

- Teti, R., Machining of Composite Materials, CIRP Annals- Manufacturing Technology, Vol. 51(2), pp.611–634, 2002
- Ventura, G. and Martelli, V., Thermal Conductivity of Kevlar 49 between 7 and 290 K, Cryogenics, Vol. 49(12), pp.735–737, 2009
- Walton, P.L. and Majumdar, A.J., Creep of Kevlar 49 Fiber and a Kevlar 49-Cement Composite, Journal of Materials Science, Vol. 18(10), pp.2939-2946, 1983
- Wang, Y., Li, J. and Zhao, D., Mechanical Properties of Fiber Glass and Kevlar Woven Fabric Reinforced Composites, Composites Engineering, Vol. 5(9), pp.1159–1175, 1995
- Wang, Y. and Xia, Y.M., The Effects of Strain Rate on the Mechanical Behavior of Kevlar Fiber Bundles: An Experimental and Theoretical Study, Composites Part A: Applied Science and Manufacturing, Vol. 29(11), pp.1411–1415, 1998
- Wu, H.F. and Yeh, J.R., Compressive Response of Kevlar-Epoxy Composites: Experimental Verification, Journal of Materials Science, Vol. 27(3), pp.755-760, 1992
- Yue, C.Y., Sui, G.X. and Looi, H.C., Effects of Heat Treatment on the Mechanical Properties of Kevlar-29 Fiber, Composites Science and Technology, Vol. 60(3), pp.421–427, 2000
- Zain, A.Z., Haron, H. and Sharif, S., Application of GA to Optimize Cutting Conditions for Minimizing Surface Roughness In End Milling Machining Process, Expert Systems with Applications, Vol. 37(6), pp.4650-4659, 2010
- Zhong, Z.W., Khoo, L.P. and Han, S.T., Prediction of Surface Roughness of Turned Surfaces Using Neural Networks, International Journal of Advanced Manufacturing Technology, Vol. 28(7-8), pp.688-693, 2006